nature communications

Article

https://doi.org/10.1038/s41467-024-55034-y

Human ANP32A/B are SUMOylated and utilized by avian influenza virus NS2 protein to overcome species-specific restriction

Received: 9 June 2024

Accepted: 28 November 2024

Published online: 30 December 2024

Check for updates

Liuke Sun[1], Xing Guo[1], Mengmeng Yu[1], Xue-Feng Wang[1], Huiling Ren[1] & Xiaojun Wang[1,2]

Human ANP32A/B (huANP32A/B) poorly support the polymerase activity of avian influenza viruses (AIVs), thereby limiting interspecies transmission of AIVs from birds to humans. The SUMO-interacting motif (SIM) within NS2 promotes the adaptation of AIV polymerase to huANP32A/B via a yet undisclosed mechanism. Here we show that huANP32A/B are SUMOylated by the E3 SUMO ligase PIAS2α, and deSUMOylated by SENP1. SUMO modification of huANP32A/B results in the recruitment of NS2, thereby facilitating huANP32A/B-supported AIV polymerase activity. Such a SUMO-dependent recruitment of NS2 is mediated by its association with huANP32A/B via the SIM-SUMO interaction module, where K68/K153-SUMO in huANP32A or K68/K116-SUMO in huANP32B interacts with the NS2-SIM. The SIM-SUMO-mediated interactions between NS2 and huANP32A/B function to promote AIV polymerase activity by positively regulating AIV vRNP-huANP32A/B interactions and AIV vRNP assembly. Our study offers insights into the mechanism of NS2-SIM in facilitating AIVs adaptation to mammals.

Influenza A viruses (IAVs) represent a significant cause of respiratory illness in both animals and humans, and pose a serious threat to human health[1]. While most influenza strains primarily circulate within avian hosts, certain highly pathogenic AIV strains (e.g., H5N1, H5N8, and H7N9) have the capacity to infect humans with potentially fatal consequences. Once these strains acquire the ability for human-to-human transmission through mutation, they may even cause influenza pandemics, presenting a substantial risk to public health. Nonetheless, the cross-species transmission of AIVs from avian hosts to mammals is limited by robust host barriers across different species[1–4]. The viral polymerase (vPol) plays a pivotal role in directing the transcription and replication of the viral genome, serving as a major determinant of the host range of IAVs[5–8]. In general, the vPol activity of AIV is severely restricted in mammalian cells, thus hindering efficient initiation of the replication process[9,10]. Recent research has elucidated that the host factors ANP32A/B, which are members of the acidic nuclear phosphoprotein 32 kDa (ANP32) family, serve as essential cofactors for the IAV polymerase. Species-specific differences in this host factor underlie the severe restriction of AIV vPol within mammalian cells. Chicken ANP32A (chANP32A) efficiently supports AIV vPol activity owing to a specific 33 amino-acid insertion, whereas mammalian ANP32A and ANP32B lack such an insertion and are unable to effectively support AIV vPol function[11]. Only AIV vPol variants that have acquired adaptive mutations (e.g., PB2-E627K, and others) can proficiently utilize mammalian ANP32A/B[11–13].

SUMOylation is a ubiquitous post-translational modification in eukaryotes that involves the covalent attachment of small ubiquitin-like modifiers (SUMO) to lysine residues on target proteins[14–16]. The mammalian SUMO family comprises four members: SUMO1, SUMO2, SUMO3 and SUMO4, with only the first three primarily participating in SUMOylation. Notably, SUMO2 shares a substantial 97% amino acid sequence similarity with SUMO3, while its similarity with SUMO1 is only 47%[14–16]. SUMO modification predominantly occurs in the nucleus and is characterized by a dynamic and reversible process. The

[1]State Key Laboratory for Animal Disease Control and Prevention, Harbin Veterinary Research Institute, The Chinese Academy of Agricultural Sciences, Harbin, China. [2]Institute of Western Agriculture, The Chinese Academy of Agricultural Sciences, Changji, China. e-mail: wangxiaojun@caas.cn

SUMOylation mechanism encompasses SUMO activating enzymes (E1), SUMO binding enzymes (E2), and SUMO ligases (E3)[14–16]. Once covalently conjugated to a target, SUMO not only exerts direct effects on target proteins but also recruits downstream effectors through the SIM-SUMO interaction pattern. This pattern involves a non-covalent interaction between SUMO and a SUMO-interacting motif (SIM) in downstream effectors[17,18]. SIMs typically feature hydrophobic cores preceded or followed by negatively charged residues. In recent years, emerging studies have unveiled the pivotal roles of SIM-SUMO interactions in various crucial cellular processes, including liquid-liquid phase separation, histone function, DNA transcription, DNA repair, the cell cycle, and diverse host-pathogen interactions[18–20].

Previous studies have shown that H5N1 NS2 exhibits avian vPol-enhancing properties[21]. We have recently demonstrated that NS2—regardless of its origin—depends on its SIM to specifically enhance the function of the avian vPol in mammalian cells, but not in avian cells, by facilitating the utilization of mammalian ANP32A/B by the avian vPol[22]. However, the precise mechanism by which the SIM in NS2 enhances mammalian ANP32A/B-supported avian vPol activity remains unclear. Our earlier discovery[22], revealing that the SIM in NS2 exhibits a preference for interacting with SUMO-conjugated proteins rather than with SUMO itself, led us to speculate whether NS2 relies on the SIM-SUMO interaction pattern to associate with either SUMOylated viral proteins or host factors, and thereby exerting its function in promoting mammalian ANP32A/B-supported AIV vPol activity. Here, we show that huANP32A/B are SUMOylated and thus are able to interact with NS2 via its SIM. SUMOylation of huANP32A/B is specifically fine-tuned by the E3 SUMO ligase PIAS2α and the deSUMOylation enzyme SENP1. NS2 uses its SIM to bind with SUMOylated huANP32A/B in the nucleus via a SIM-SUMO interaction pattern. This then increases huANP32A/B-supported avian vPol activity by facilitating vRNP-huANP32A/B interactions and avian vRNP assembly. We also identified that SUMOylation of huANP32A at K68/K153 or huANP32B at K68/K116 appears to be required for their association with NS2. Impairment of the SIM-SUMO mediated interactions between NS2 and huANP32A/B results in reduction of avian vPol activity and AIV replication. Thus, SIM-SUMO-mediated interactions between viral proteins and host factors represent a new regulatory mechanism for the function of avian vPol in human cells and, therefore, also for the adaptation of AIVs.

Results

NS2 relies on its SIM to interact with huANP32A/B

To identify SUMOylated factors that interact with NS2 via SIM-SUMO interaction pattern, as proposed in our previous study[22], Flag-tagged H9N2-NS2 or an empty vector were transfected into HEK293T cells. After transfection for 24 hours, the cells were infected with avian H9N2 virus for an additional 24 hours followed by immunoprecipitation (IP) using anti-Flag beads (Fig. 1a). The purified protein complexes were analyzed using immunoblotting assays or liquid chromatography-tandem mass spectrometry (LC-MS/MS). Notably, huANP32A/B were exclusively identified in Flag-H9N2-NS2-derived samples and not in control samples (Fig. 1b). Interestingly, several previous large-scale proteomic analyses of SUMOylated proteins have identified huANP32A/B as potential SUMOylation substrates[23–26]. Consequently, we hypothesized that the host factors ANP32A/B are promising candidates.

We next examined whether H9N2-NS2 could directly bind to huANP32A or huANP32B. Co-immunoprecipitation (Co-IP) and immunoblotting assays demonstrated that both endogenous huANP32A and huANP32B were co-immunoprecipitated with Flag-H9N2-NS2 in HEK293T cells (Fig. 1c). Furthermore, a reciprocal Co-IP experiment indicated that both huANP32A-Flag and huANP32B-Flag could co-precipitate with GST-tagged H9N2-NS2, but not with GST alone (Fig. 1d). Additionally, direct interactions between H9N2-NS2 and huANP32A/B were confirmed in a Proximity Ligation Assay (PLA) under avian H9N2 virus infection conditions in HEK293T cells (Fig. 1e). The interaction between H9N2-NS2 and huANP32A/B was further validated using bimolecular fluorescence complementation (BiFC) assays, where NS2 and huANP32A/B were expressed as fusion proteins with the N- and C-terminal halves of the Venus protein, respectively (Fig. 1f). When VN-NS2 and huANP32A/B-VC were expressed individually in HEK293T cells, no fluorescence signals were detected via confocal microscopy. However, strong reconstituted fluorescence signals, primarily in the nucleus, were observed when VN-NS2 was paired with huANP32A-VC or huANP32B-VC (Fig. 1g). Based on these results, H9N2-NS2 may interact directly with host factors huANP32A/B in the nucleus.

To further investigate whether the SIM of NS2 is necessary for its interaction with huANP32A/B, we utilized a SIM-defective mutant of NS2. This mutant (NS2-VE/GG) contains two glycine substitutions (V109G and E110G, VE/GG) in the core region of NS2-SIM, as described in a previous report[22]. The mutant was analyzed for its binding with huANP32A/B in a Co-IP assay. Interestingly, compared to wild-type NS2 (NS2-WT), NS2-VE/GG exhibited reduced interactions with both huANP32A and huANP32B (Fig. 1h). The diminished interaction between NS2-VE/GG and huANP32A/B was further confirmed using BiFC assays. The VN-NS2-VE/GG construct was co-expressed with huANP32A-VC or huANP32B-VC in HEK293T cells. As shown in Fig. 1i-k, notably faint BiFC signals were detected from the VN-NS2-VE/GG and huANP32A-VC pairs and from the VN-NS2-VE/GG and huANP32B-VC pairs. Additionally, we obtained similar results when using another previously described SIM-defective mutant of NS2[22], which contains only one glycine substitution (E110G) in the core region of SIM (Supplementary Fig. 1). These results further confirm that NS2 relies on its SIM to efficiently interact with huANP32A/B.

These results collectively demonstrate that the SIM of NS2 plays a crucial role in mediating its interaction with huANP32A/B within the nucleus.

Human ANP32A and ANP32B are SUMOylated by SUMO1, SUMO2 and SUMO3

To determine whether huANP32A/B are SUMOylated and whether this SUMOylation is influenced by AIV infection, we initially investigated whether huANP32A and huANP32B serve as authentic SUMOylation substrates. To this end, we conducted SUMOylation assays by transfecting HEK293T cells with huANP32A-HA, Myc-Ubc9, and either His-SUMO1/2/3 or their non-conjugatable forms (His-SUMO1m/2 m/3 m) carrying G-A mutations at the two C-terminal glycine residues crucial for conjugation. Following enrichment of SUMOylated proteins via histidine affinity under denaturing conditions, immunoblot analysis using an anti-HA antibody revealed three clear bands above 40 kDa for huANP32A upon overexpression of His-SUMO1/2/3, but not with His-SUMO1m/2 m/3 m (Fig. 2a, left). Given that the molecular weights of HA-tagged huANP32A and SUMO1/2/3 are ~33 kDa and ~15-20 kDa, respectively, we speculated that huANP32A underwent modification by at least two SUMO moieties. Subsequently, we conducted SUMOylation assays with an huANP32B-HA construct, revealing that huANP32B could indeed undergo SUMOylation. The pattern of SUMOylated species was the same as that of huANP32A, suggesting that at least two sites in huANP32B were modified by SUMOylation (Fig. 2a, right). To further substantiate these findings, we demonstrated that endogenous huANP32A/B were also SUMOylated. As shown in Fig. 2b, SUMOylated species of endogenous huANP32A and huANP32B were readily detected in HEK293T cells. No band corresponding to SUMOylated huANP32A/B was observed in HEK293T-TKO cells, where the *huANP32A*, *huANP32B* and *huANP32E* genes were knocked out using CRISPR/Cas9 technology, as described in our previous studies[27], further verifying the specificity of the antibodies used against endogenous ANP32A and ANP32B. These results suggest that all three SUMO isoforms are covalently conjugated to huANP32A and huANP32B in HEK293T cells.

https://doi.org/10.1038/s41467-024-55034-y

Protein Name	Uniprot Accession	Unique Peptides	Hit by Flag-NS2 replicates (n=3)	Hit by Vector control replicates (n=3)
ANP32A	P39687	1	2	0
ANP32B	Q92688	1	3	0

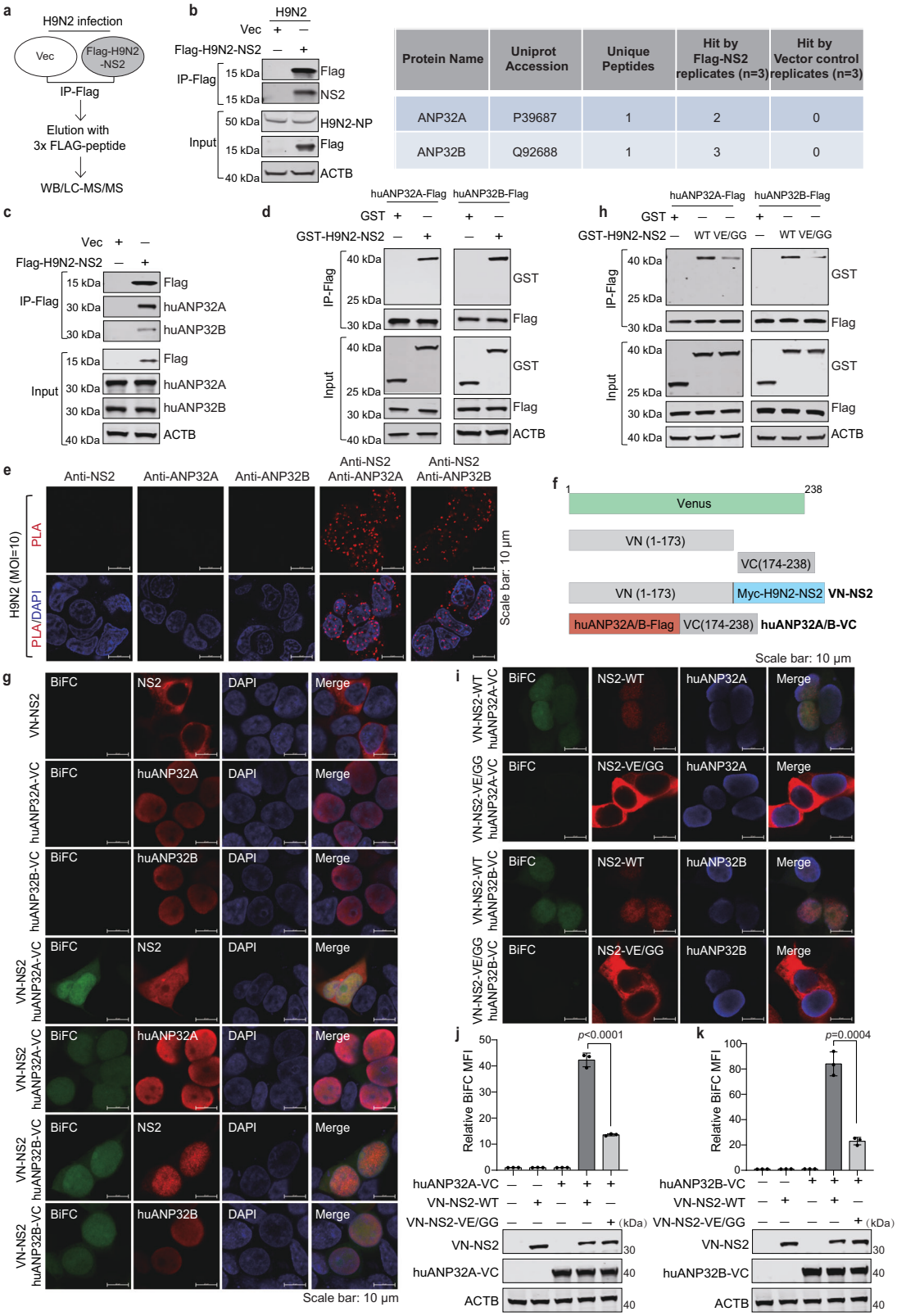

Previous studies have demonstrated that mammalian-adapted IAV infection not only contributes to a global increase in the level of SUMOylation in host cells[24,25,28], but also specifically increases huANP32A/B SUMOylation levels[24,25]. To examine whether this also occurs during AIV infection, HEK293T cells were first infected with different doses of avian H9N2 virus for 24 hours, after which the cells were collected for immunoblotting assays. As shown in Fig. 2c, H9N2 infection also results in a global increase in SUMOylation levels in host cells. To further investigate where H9N2 infection specifically enhances the SUMOylation levels of huANP32A and huANP32B, HEK293T cells were transfected with HA-tagged huANP32A or huANP32B along with His-SUMO1 or its non-conjugatable form (His-SUMO1m). Following a 24-hour transfection period, the cells were subsequently infected with or without avian H9N2 virus for an

Fig. 1 | NS2 relies on its SIM to interact with huANP32A/B. a Schematic representation of the experimental design for analyzing H9N2-NS2 interacting proteins via LC-MS/MS proteomics. **b** HEK293T cells were transfected with Flag-H9N2-NS2 or an empty vector (Vec) control. After 24 hours, the cells were infected with H9N2 virus at a multiplicity of infection (MOI) of 0.01. Twenty-four hours post-infection, cells were harvested for immunoprecipitation (IP) using anti-Flag beads. Protein complexes were eluted with 3× Flag peptides and analyzed by western blotting (WB) (left) or LC-MS/MS (right), with $n = 3$ independent biological replicates. **c** Co-IP experiments showing the interaction of Flag-H9N2-NS2 with endogenous huANP32A/B in HEK293T cells. **d** Co-IP experiments showing the interaction of H9N2-NS2 with exogenous huANP32A/B in HEK293T-TKO cells stably expressing huANP32A-Flag or huANP32B-Flag. **e** Direct interaction between NS2 from H9N2 infection and huANP32A/B was measured using a proximity ligation assay (PLA) in HEK293T cells, with controls using one antibody. The PLA was performed 24 hours post-infection. **f** Schematic representation of the BiFC fusion proteins. **g** Confocal experiments using a BiFC assay showing the interaction of NS2 with huANP32A/B in HEK293T cells. **h** Co-IP experiments showing that mutations (V109G and E110G, VE/GG) in NS2-SIM suppressed its interaction with huANP32A/B in HEK293T-TKO cells that stably express huANP32A-Flag or huANP32B-Flag. **i** Confocal experiments using a BiFC assay showing that VE/GG mutations in NS2-SIM suppress its interaction with huANP32A or huANP32B. **j**, **k** Flow cytometry analysis using a BiFC assay showing that NS2 interacts with huANP32A (**j**) or huANP32B (**k**) depending on its SIM. Plasmids were transfected individually or in pairs into HEK293T cells. After 24 hours, the mean fluorescence intensity (MFI) of BiFC signals was measured by flow cytometry and are presented as relative values to the signal from untransfected cells. Western blots showing the protein expression of the indicated plasmids in HEK293T cells. Error bars represent means ± SD from $n = 3$ independent biological replicates; Statistical significance was determined by two-tailed unpaired *t-test*. Experiments in (**c**), (**d**), and (**h**) were repeated three times with consistent results. Source data are provided as a Source Data file.

additional 24 hours. The SUMOylation of huANP32A/B was then assessed through SUMOylation assays. As shown in Fig. 2d, the SUMOylation of both huANP32A and huANP32B exhibited an increase upon avian H9N2 virus infection.

Collectively, these findings conclusively establish that both huANP32A and huANP32B act as targets for SUMOylation, and that their SUMOylation modifications are positively regulated by AIV infection.

SUMOylation of huANP32A/B was controlled by the deSUMOylating enzyme SENP1 and the E3 SUMO ligase PIAS2α

SUMOylation represents a dynamic and reversible cellular process governed by deSUMOylating enzymes, and sentrin-specific proteases (SENPs) are the major deSUMOylating enzymes in mammalian cells[29]. To pinpoint the specific SUMO proteases responsible for the deSUMOylation of huANP32A/B, we co-transfected all known human nuclear SUMO-specific proteases (SENP1-3, SENP5-7, and USPL1) with huANP32A-HA or huANP32B-HA, along with Myc-Ubc9 and His-SUMO1, into HEK293T cells. Levels of huANP32A/B SUMOylation were then assessed through SUMOylation assays. We observed that co-expression of SENP1 and SENP2 notably decreased huANP32A/B SUMOylation (Fig. 3a, b). Immunofluorescence staining revealed that SENP1, but not SENP2, co-localized with huANP32A or huANP32B in the nucleus (Fig. 3c). Consequently, we focused on addressing the role of SENP1 in huANP32A/B deSUMOylation. To substantiate this role, we investigated the interaction between SENP1 and huANP32A or huANP32B in HEK293T cells. As shown in Fig. 3d, e, Flag-SENP1 specifically interacts with both the exogenous huANP32A/B (Fig. 3d) and the endogenous huANP32A/B (Fig. 3e). Additionally, direct interactions between endogenous SENP1 and endogenous huANP32A/B were confirmed using a Proximity Ligation Assays (PLA) in HEK293T cells (Fig. 3f). Most importantly, depletion of endogenous SENP1 led to a considerable enhancement of huANP32A/B SUMOylation (Fig. 3g). These findings indicate that SENP1 targets huANP32A/B for deSUMOylation.

The primary SUMO E3 ligases in mammalian cells belong to the PIAS family proteins[30]. The human PIAS gene family is known to comprise four members: PIAS1, PIASx (also known as PIAS2), PIAS3 and PIASy (also known as PIAS4), with PIAS2 existing in two isoforms (PIAS2α and PIAS2β). To determine the putative E3 SUMO ligase for huANP32A/B SUMOylation, His-SUMO1 and each of the five PIAS family members were co-transfected with huANP32A-HA or huANP32B-HA into HEK293T cells, and huANP32A/B SUMOylation was assessed by performing SUMOylation assays. Of the tested isoforms, PIAS2α prominently enhanced huANP32A/B SUMOylation, while the other PIAS variants did not exhibit any such effects (Fig. 3h, i). Additionally, PIAS2α specifically colocalized with huANP32A/B in the nucleus (Fig. 3j). We further confirmed the specific interaction between Flag-PIAS2α and both exogenous huANP32A/B (Fig. 3k) and endogenous huANP32A/B (Fig. 3l). Moreover, the PIAS2-huANP32A/B interactions at the endogenous level in HEK293T cells were validated using a Proximity Ligation Assay (PLA) (Fig. 3m). Depletion of endogenous PIAS2 resulted in defects in huANP32A/B SUMOylation (Fig. 3n; Supplementary Fig. 2). These results clearly indicate that PIAS2α plays a crucial role in directing huANP32A/B for SUMOylation.

These findings collectively establish that both huANP32A and huANP32B undergo SUMOylation catalyzed by the SUMO E3 ligase PIAS2α and subsequent deSUMOylation mediated by SENP1.

NS2 engages with huANP32A/B via a SIM-SUMO dependent manner

To explore the impact of huANP32A/B SUMOylation on their interactions with NS2, we investigated whether the huANP32A/B-NS2 interactions were affected by the alterations in huANP32A/B SUMOylation levels. This was achieved by overexpressing the single SUMO E2 conjugating enzyme (Ubc9), employing the targeted deSUMOylation enzyme SENP1 for huANP32A/B SUMOylation, or by administering a selective inhibitor of the SUMOylation enzymatic cascade (TAK-981). As shown in Fig. 4a, co-expression of Ubc9 led to a substantial increase in huANP32A/B SUMOylation. Consequently, Ubc9 heightened the huANP32A/B-NS2 interactions (Fig. 4b, c). Conversely, co-expression of SENP1 diminished huANP32A/B SUMOylation (Fig. 4d), thereby inhibiting the interaction of huANP32A/B with NS2 (Fig. 4e). Moreover, TAK-981 treatment not only impeded huANP32A SUMOylation but also disrupted the huANP32A-NS2 interaction (Fig. 4f, g). These findings unequivocally underscore the crucial role of huANP32A/B SUMOylation in facilitating their association with NS2.

Collectively, the above results demonstrate that the interactions between huANP32A/B and NS2 rely on the canonical SIM-SUMO interaction module, where SUMO attached to huANP32A/B interacts with the SIM on NS2 (Fig. 4h).

SIM-SUMO interactions between NS2 and huANP32A/B are required for the avian vPol-enhancing function of NS2

We next intended to assess the necessity of SIM-SUMO-mediated NS2-huANP32A/B interactions for the avian vPol-enhancing function of NS2. To this end, we proceeded to directly assess whether disruption of these interactions, achieved through either the destabilization of NS2-SIM integrity or inhibition of huANP32A/B SUMOylation, would affect the ability of NS2 in promoting huANP32A/B-supported avian vPol activity (Fig. 5a). As shown in Fig. 5b, c, disruption of NS2-SIM integrity caused NS2 to lose its avian vPol-enhancing properties in HEK293T-TKO cells reconstituted with either huANP32A or huANP32B, which is consistent with our previous study[22]. These results support the hypothesis that the SIM-SUMO-mediated interactions between NS2 and huANP32A/B are indispensable for the ability of NS2 to enhance huANP32A/B-supported avian vPol activity.

https://doi.org/10.1038/s41467-024-55034-y

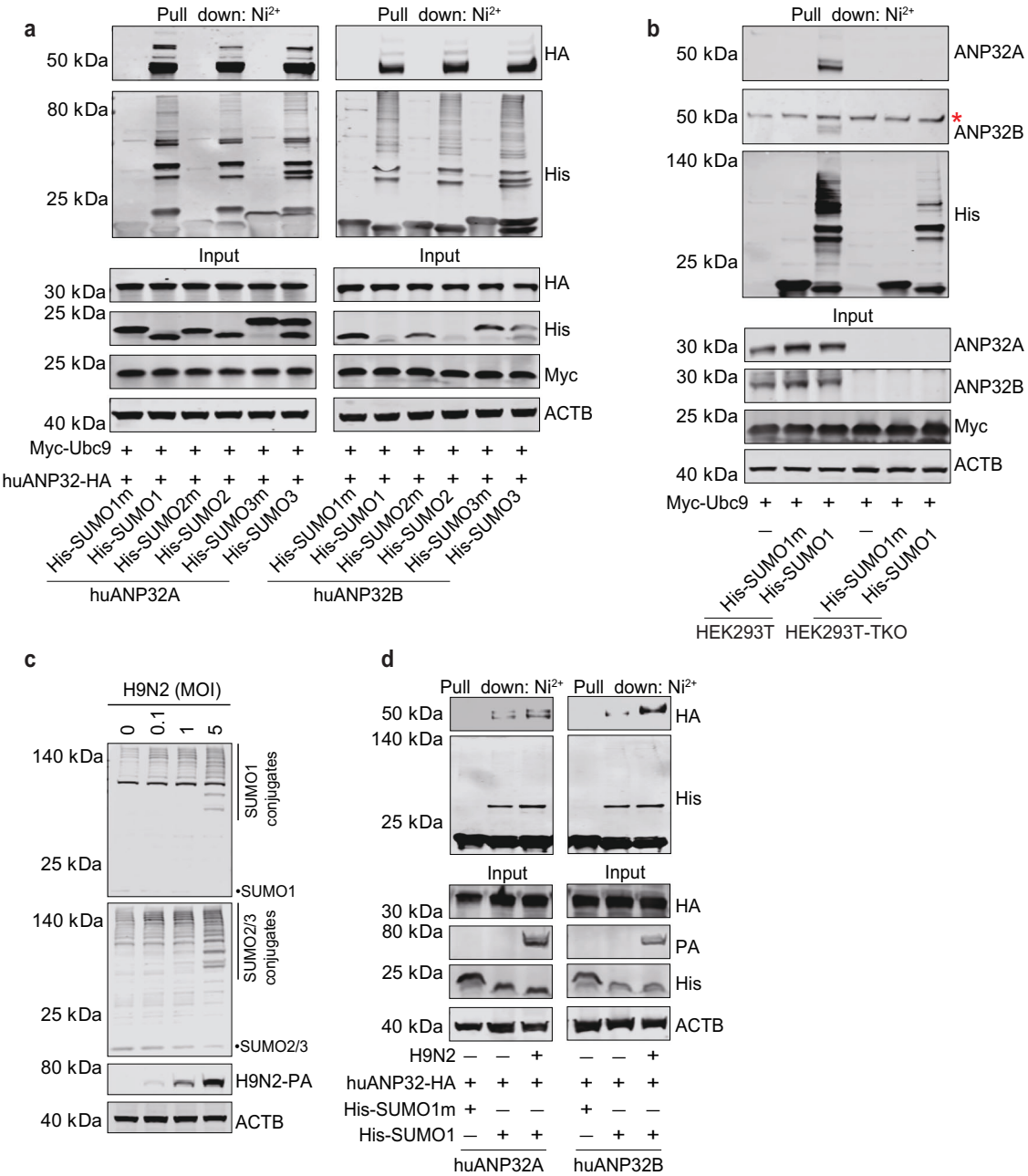

Fig. 2 | SUMOylation of huANP32A/B is regulated by H9N2 infection. a Ni^{2+}-NTA bead affinity pull-down assay results showing the modification of exogenous huANP32A (left) and huANP32B (right) with SUMO1, SUMO2, and SUMO3 in HEK293T cells. **b** Ni^{2+}-NTA bead affinity pull-down assay results showing the modification of endogenous huANP32A and huANP32B with SUMO1 in HEK293T cells. *indicates non-specific protein band. **c** Western blot analysis showing that H9N2 virus infection upregulates the global SUMOylation level in HEK293T cells. **d** Ni^{2+}-NTA bead affinity pull-down assay results showing that the SUMOylation of huANP32A (left) or huANP32B (right) in HEK293T cells was notably enhanced by H9N2 AIV infection. HEK293T cells were transfected with the indicated plasmids for 24 hours followed by H9N2 AIV infection (MOI = 0.01) for another 24 hours. Cells were then harvested for SUMOylation assays and immunoblotting analysis. In (**a** to **d**), experiments were independently repeated three times with consistent results. Source data are provided as a Source Data file.

We then proceeded to investigate the impact of inhibiting SIM-SUMO interactions on the ability of NS2 to enhance the activity of huANP32A/B-supported avian vPol by reducing huANP32A/B SUMOylation levels. To achieve this, we engineered a SUMOylation-deficient mutant of huANP32A, denoted as huANP32A-K0, with lysine-to-arginine substitutions at all sixteen lysine residues of the protein. Similarly, a counterpart mutant of huANP32B, termed huANP32B-K0, was generated with lysine-to-arginine substitutions at all seventeen lysine residues (Fig. 5d). Theoretically, huANP32A/B-K0 should lose its capability to be SUMOylated and would therefore be unable to engage in the SIM-SUMO interaction mode crucial for interacting with NS2. As we expected, the SUMOylation assays we conducted in HEK293T cells confirmed that neither huANP32A-K0 nor huANP32B-K0 were able to undergo SUMOylation (Fig. 5e). Subsequent polymerase activity assays performed in HEK293T-TKO cells revealed a significant reduction in the ability of NS2 to enhance H9N2 and H7N9 (PB2-627E) vPol activity when supported by huANP32A/B-K0 compared to wild-type huANP32A/B (Fig. 5f, g).

To evaluate whether the observed changes in polymerase activity correlate with viral replication, we firstly established MDCK-

https://doi.org/10.1038/s41467-024-55034-y

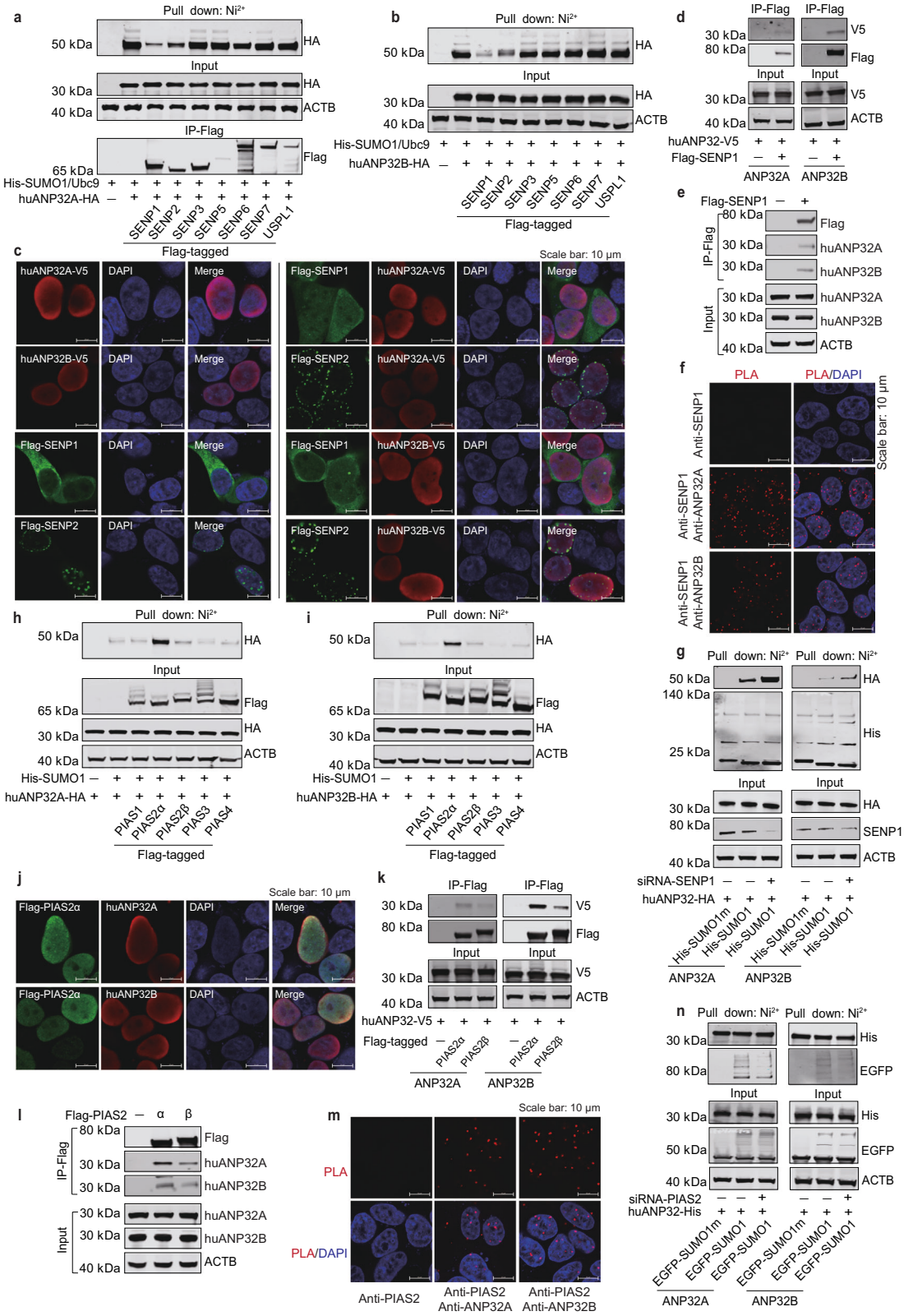

TKO cells by knocking out the triple canine *ANP32A*, *ANP32B*, and *ANP32E* genes using CRISPR-Cas 9 technology (Supplementary Fig. 3). Multi-cycle replication assays of avian H9N2 virus were then subsequently conducted in MDCK-TKO cells reconstituted with empty vector, huANP32A-WT or huANP32A-K0, respectively. Notably, virus growth kinetics revealed that huANP32A-K0 has lost its ability to support the replication of avian H9N2 viruses (Fig. 5h). Western blot analysis confirmed the equal expression of huANP32A proteins in these transfected cells (Fig. 5i). We performed similar experiments for huANP32B and huANP32B-K0 and obtained similar observations that huANP32B-K0 failed to support the replication of avian H9N2 viruses (Fig. 5j, k).

To further confirm that the reduced ability of NS2 to enhance the vPol activity of H9N2 and H7N9 (PB2-627E) when supported by

https://doi.org/10.1038/s41467-024-55034-y

Fig. 3 | SUMOylation of huANP32A/B is regulated by the deSUMOylase SENP1 and the SUMO E3 ligase PIAS2α. a, **b** Ni^{2+}-NTA bead affinity pull-down assay results showing that the SUMOylation of huANP32A (**a**) or huANP32B (**b**) in HEK293T cells was notably reduced by overexpression of SENP1 or SENP2. **c** Immunofluorescent staining showing that Flag-SENP1 was co-localized with huANP32A/B-V5 in the nucleus, whereas Flag-SENP2 was not. **d**, **e** Co-IP experiments showing the interaction of Flag-SENP1 with exogenous huANP32A/B (**d**) and the endogenous huANP32A/B (**e**). **f** The interactions between SENP1 and huANP32A/B at the endogenous level were confirmed using a proximity ligation assay (PLA) in HEK293T cells. **g** Ni^{2+}-NTA bead affinity pull-down assay results showing that knockdown of endogenous SENP1 enhanced the huANP32A/B SUMOylation level in HEK293T cells. **h**, **i** Ni^{2+}-NTA bead affinity pull-down assay results showing that the SUMOylation of huANP32A (**h**) or huANP32B (**i**) in HEK293T cells was notably enhanced by overexpression of PIAS2α. **j** Co-localization of huANP32A/B-V5 with Flag-PIAS2α was analyzed using immunofluorescence staining. **k**, **l** Co-IP experiments showing the interaction of Flag-PIAS2α with exogenous huANP32A/B (**k**) and the endogenous huANP32A/B (**l**). **m** The PIAS2-huANP32A/B interactions at the endogenous level were confirmed using a proximity ligation assay (PLA) in HEK293T cells. **n** Ni^{2+}-NTA bead affinity pull-down assay results showing that knockdown of endogenous PIAS2 reduced the SUMOylation of huANP32A/B in HEK293T cells. All Western blot experiments were independently repeated at least twice with consistent results. Source data are provided as a Source Data file.

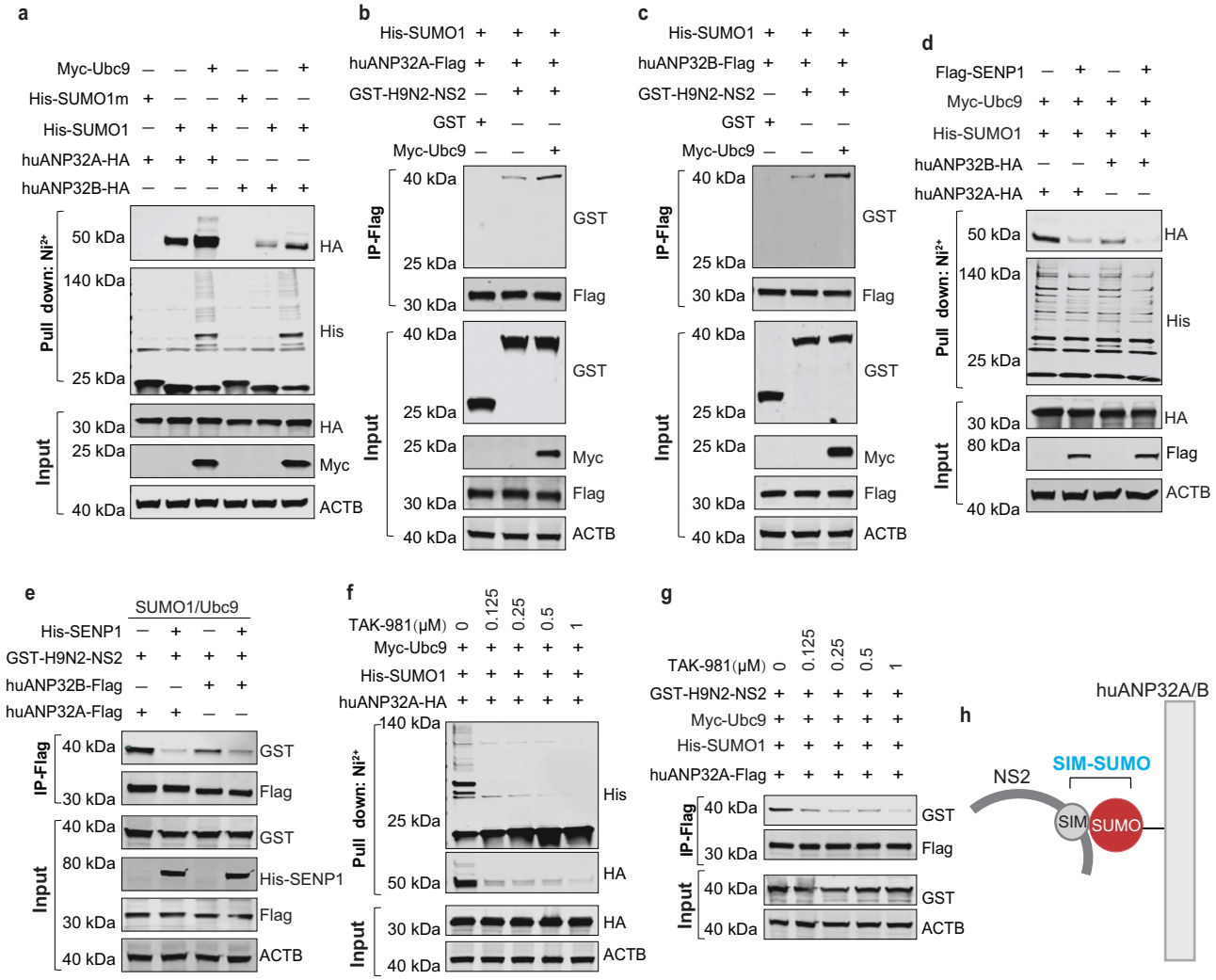

Fig. 4 | SUMOylation of huANP32A and huANP32B determine their association with NS2. a Ni^{2+}-NTA bead affinity pull-down assay results showing that SUMOylation of huANP32A or huANP32B in HEK293T cells was enhanced by overexpression of Ubc9. **b**, **c** Co-IP experiments showing that overexpression of Ubc9 promoted the interaction between H9N2-NS2 and huANP32A (**b**) or huANP32B (**c**). **d** Ni^{2+}-NTA bead affinity pull-down assay results showing that SUMOylation of huANP32A or huANP32B in HEK293T cells was reduced by overexpression of SENP1. **e** Co-IP experiments showing overexpression of SENP1 suppressed the interaction between H9N2-NS2 and huANP32A or huANP32B. **f** Ni^{2+}-NTA bead affinity pull-down assay results showing the SUMOylation of huANP32A in HEK293T cells was reduced by treatment with TAK-981. **g** Co-IP experiments showing that treatment with TAK-981 suppressed NS2-huANP32A interaction. **h** Illustration of the interaction model between NS2 and huANP32A/B mediated by the SIM-SUMO working pattern. All Western blot experiments were independently repeated at least twice with consistent results. Source data are provided as a Source Data file.

huANP32A/B-K0 is not a direct result of huANP32A/B-K0 losing its function due to the loss of its natural fold, we next compared its capacity to support the polymerase activity of influenza B virus (IBV) with that of the wild type. We chose the IBV polymerase for these experiments for two reasons. First, like the IAV polymerase, the function of the IBV polymerase also relies on the host factors ANP32A/B[27]. Second, the SIM present in IAV NS2 is not conserved in IBV NS2[22], therefore, we assume that there is no SIM-SUMO-mediated interaction between IBV NS2 and huANP32A/B, as observed for IAV NS2 and huANP32A/B. As shown in Supplementary Fig. 4, huANP32A/B-K0 retains a similar ability to that of the wild type in supporting IBV polymerase activity, indicating that huANP32A/B-K0 still maintains its

https://doi.org/10.1038/s41467-024-55034-y

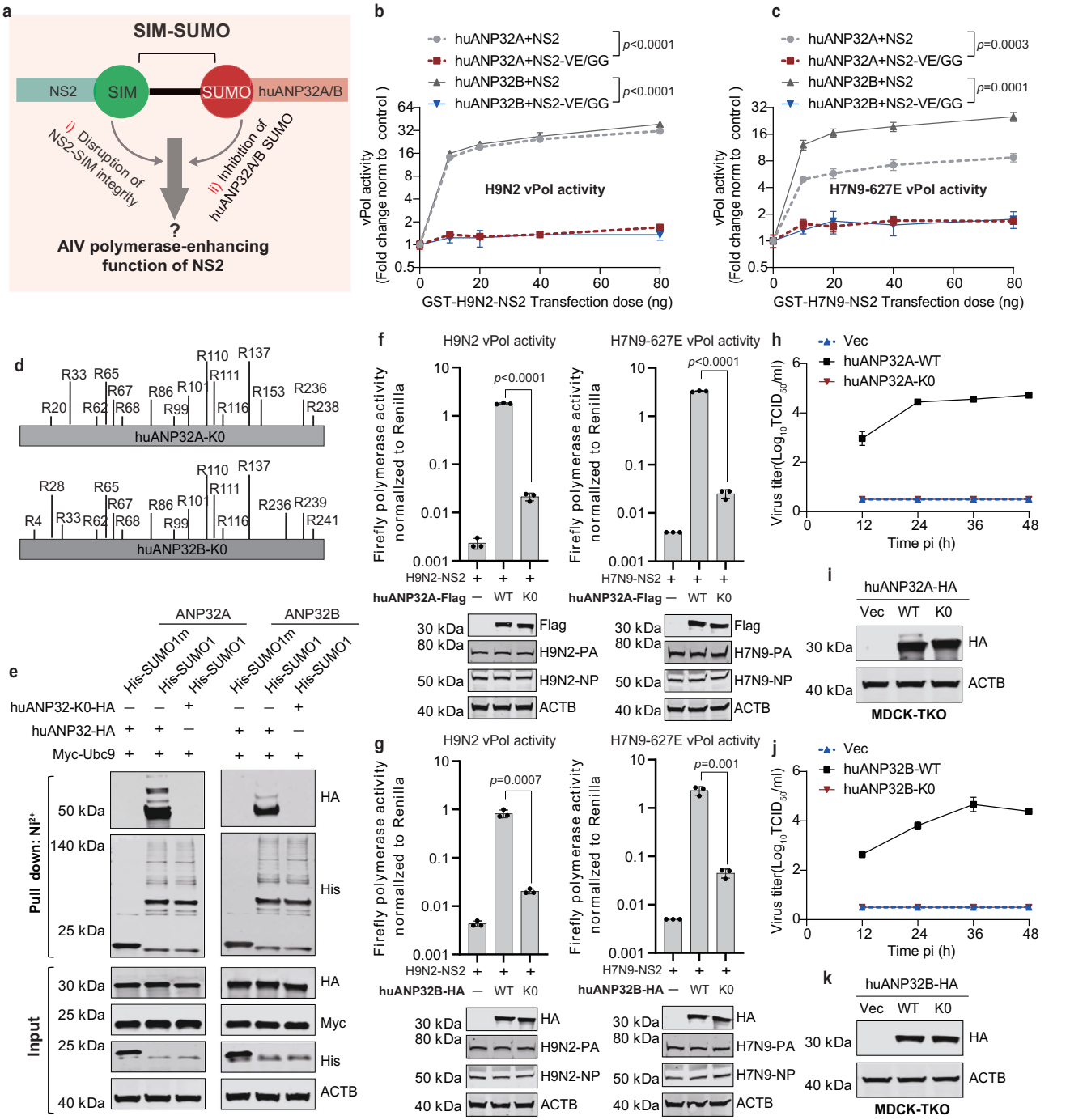

Fig. 5 | The function of NS2-SIM in enhancing huANP32A/B-supported avian vPol activity depends on its interaction with huANP32A/B via the SIM-SUMO working pattern. a Schematic illustrating two strategies employed for the investigation of whether the SIM-SUMO-mediated interactions between NS2 and huANP32A/B are required for NS2-SIM to promote huANP32A/B-supported AIV vPol activity. **b**, **c** Minigenome assays in HEK293T-TKO cells showing that disruption of the H9N2 or H7N9 NS2-SIM integrity impairs the ability of NS2 to enhance huANP32A/B-supported H9N2 (**b**) or H7N9 (PB2-627E) (**c**) vPol activity, respectively. **d** Schematic model of the generation of lysine-free mutant of huANP32A/B (huANP32A/B-K0). **e** Ni^{2+}-NTA bead affinity pull-down assay results showing that huANP32A/B-K0 could not be SUMOylated in HEK293T cells. **f**, **g** Minigenome assays in HEK293T-TKO cells showing that the ability of NS2 to promote huANP32A-K0 (**f**) or huANP32B-K0 (**g**)-supported H9N2 or H7N9 (PB2-627E) vPol activity was greatly reduced. The accompanying western blots show the expression of ANP32A-Flag/ANP32B-HA constructs and vRNP components (PA/NP). **h** Replication kinetics of avian H9N2 virus. MDCK-TKO cells or those tranfected with huANP32A-HA or huANP32A-K0-HA were infected (MOI = 0.01), and viral titers were determined at the indicated time points. **i** Western blots showing equal expression of HA-tagged ANP32A in transfected MDCK-TKO cells. **j** The replication kinetics of avian H9N2 virus were assessed in MDCK-TKO cells transfected with either empty vector, huANP32B-HA or huANP32B-K0-HA (MOI = 0.01). Viral titers were determined at the indicated time points. **k** Western blots showing equal expression of HA-tagged ANP32B in transfected MDCK-TKO cells. In (**b**), (**c**), (**f** to **h**) and (**j**), error bars represent mean ± SD from $n = 3$ independent biological replicates; Statistical significance was determined by two-way ANOVA (**b** and **c**) or two-tailed unpaired *t-test* (**f** and **g**). Experiments in (**e**) were independently repeated three times with consistent results. Source data are provided as a Source Data file.

natural fold and retains certain biological functions necessary for influenza viral polymerase activity.

Taken together, these results demonstrate that disruption of either huANP32A/B SUMO or NS2 SIM sites attenuates their interaction and impairs huANP32A/B-supported AIV polymerase activity. This highlights the crucial role of SIM-SUMO-mediated interactions between NS2 and huANP32A/B in facilitating NS2 function in promoting AIV polymerase activity, especially when supported by huANP32A/B.

SUMOylation of huANP32A at K68/K153 sites determines its association with NS2

Human ANP32A comprises sixteen lysine residues. Our objective was to pinpoint the primary site for huANP32A SUMOylation crucial for its association with NS2. Given that the SIM-SUMO-mediated interactions between NS2 and huANP32A/B are required for NS2 to promote huANP32A/B-supported avian vPol activity, it is reasonable to expect that reintroducing into huANP32A-K0 the major SUMOylation site present in wild-type huANP32A, which determines its association with NS2, will enhance the support of avian vPol activity by huANP32A-K0 in the presence of NS2. To explore this, a series of huANP32A-K0 mutants were generated, in which each of the sixteen lysines present in wild-type huANP32A was individually mutated back (R-to-K) into the huANP32A-K0 construct. Western blot analysis confirmed comparable expression levels of all indicated constructs (Supplementary Fig. 5). Subsequently, these huANP32A-K0 constructs were assessed for their ability to support avian vPol activity by performing polymerase activity assays in HEK293T-TKO cells. The results revealed that in the presence of NS2, four mutants, huANP32A-K0-R68K, huANP32A-K0-R116K, huANP32A-K0-R153K and huANP32A-K0-R236K, supported H9N2 vPol activity to a greater extent than huANP32A-K0, indicating that SUMOylation at sites K68, K153, K116 and K236 in huANP32A is crucial for its interaction with NS2-SIM (Fig. 6a). In comparison to the other three mutations, the R236K mutation exhibited the weakest impact on polymerase activity, resulting in less than a 1-fold effect. Consequently, the R236K mutation was excluded from subsequent experiments. Double, and triple R-to-K mutations at these sites were then further introduced into huANP32A-K0 constructs (Fig. 6b), and these modified constructs were individually reconstituted into HEK293T-TKO cells for polymerase activity assays. As shown in Fig. 6c, d, double (R68K/R153K) and triple (R68K/R116K/R153K) point mutants supported significantly higher levels of H9N2 and H7N9 vPol activity compared to single point mutants, including R68K and R153K. However, the introduction of the R116K mutation into double mutants (R68K/R153K) did not further enhance its ability to support avian vPol activity, suggesting that K68 and K153 are the two major sites for SUMOylation in huANP32A that determine its association with NS2. Additionally, by establishing two different MDCK-TKO cell lines stably expressing either Flag-tagged huANP32A-K0 or huANP32A-K0-R68K/R153K, we observed that avian H9N2 viruses failed to establish a productive infection in either control MDCK-TKO cells or MDCK-TKO cells expressing Flag-tagged huANP32A-K0. However, MDCK-TKO cells expressing Flag-tagged huANP32A-K0-R68K/R153K efficiently supported the replication of avian H9N2 viruses (Fig. 6e, f).

The above functional experiments suggest that the K68/K153 SUMO modification in huANP32A is responsible for its association with NS2 and that this interaction is critical for the avian vPol-enhancing function of NS2. We next aim to provide further evidence to support this hypothesis.

First, we assessed whether the K68 and K153 sites in huANP32A act as authentic SUMOylation sites through SUMOylation assays. For this purpose, HEK293T-SENP1-KO cells were co-transfected with His-SUMO1, Myc-Ubc9, huANP32A-K0-HA, and its various mutants. Forty-eight hours post-transfection, cell lysates were prepared for SUMOylation assays. As shown in Fig. 6g, a signal band near 50 kDa was observed for huANP32A-K0-R68K and huANP32A-K0-R153K, but not for huANP32A-K0, indicating that K68 and K153 are SUMOylation sites for huANP32A. Additionally, we included a non-SUMOylated lysine (K86) and a highly SUMOylated lysine (K137) in these experiments to further validate the specificity of the detected SUMOylation band. However, the reason for the slower migration of huANP32A-K0-R153K-SUMO and huANP32A-K0-R137K-SUMO compared to huANP32A-K0-R68K-SUMO remains unclear and warrants further investigation.

Second, Co-IP assays demonstrated that the K68R/K153R mutations in huANP32A impaired its interaction with NS2 (Fig. 6h). Third, subsequent polymerase activity assays performed in HEK293T-TKO cells revealed that the ability of huANP32A-K68R/K153R to support avian vPol activity is significantly lower than that of wild-type huANP32A in the presence of NS2 (Fig. 6i, j). Multi-cycle replication assays of avian H9N2 virus conducted in MDCK-TKO cells further confirmed the observed changes in polymerase activity correlate with viral replication (Fig. 6k, l). Notably, the K86R and K137R mutations in huANP32A did not affect its interaction with NS2 (Fig. 6h), nor did they hinder NS2's ability to enhance huANP32A-supported AIV vPol activity (Fig. 6i, j). Given that K137 in huANP32A serves as a SUMOylation site (Fig. 6g), we conclude that only site-specific SUMOylation in huANP32A can be recognized by the NS2-SIM.

Interestingly, the K68R/K153R mutations did not affect the overall level of huANP32A SUMOylation (Supplementary Fig. 6a). This phenomenon implies compensatory effects in huANP32A SUMOylation upon introducing the K68R/K153R mutations, further supporting our hypothesis that only site-specific SUMOylation in huANP32A can be recognized by the SIM in NS2. Importantly, sequence alignments revealed that the K68 and K153 sites are well-conserved among ANP32A proteins from other mammalian species (Supplementary Fig. 7). Immunofluorescence staining showed that both huANP32A-WT and the huANP32A-K68R/K153R mutant were predominantly localized in the nucleus (Supplementary Fig. 8a).

Taken together, these findings strongly suggest that SUMOylation at K68/K153 sites of huANP32A mediates its interaction with the SIM in NS2, which is essential for NS2 to promote avian vPol activity when supported by huANP32A.

SUMOylation of huANP32B at K68/K116 sites determines its association with NS2

To pinpoint the essential sites of SUMOylation in huANP32B crucial for its association with NS2, we employed the same experimental approach as for huANP32A. As shown in Fig. 7a and Supplementary Fig. 9, both the R68K and R116K mutations markedly enhanced the ability of huANP32B-K0 to support H9N2 vPol activity in the presence of H9N2-NS2. Subsequently, we found that the double point mutant (R68K/R116K) supported H9N2 and H7N9 (PB2-627E) vPol activity to a significant extent when compared to single point mutants, including R68K and R116K (Fig. 7b–d), Additionally, these alterations in polymerase activity were mirrored in viral replication, as the introduction of the R68K/R116K mutation into huANP32B-K0 reinstated its ability to support the replication of avian H9N2 viruses (Fig. 7e, f). These functional experiments indicate that the K68/K116-SUMO modification in huANP32B is responsible for its interaction with NS2. This interaction is essential for the role of NS2 in enhancing huANP32B-supported avian vPol activity. We now intend to further validate this hypothesis using the same experimental approach as employed for huANP32A.

First, SUMOylation assays conducted in HEK293T-SENP1-KO cells confirmed that K68 and K116 serve as the sites for SUMOylation in huANP32B (Fig. 7g). In these experiments, a non-SUMOylated lysine (K67) and a highly SUMOylated lysine (K137) were included to further validate the specificity of the detected SUMOylation band. Second, Co-IP assays demonstrated that the K68R/K116R mutations in huANP32B impaired its interaction with NS2 (Fig. 7h). Third, polymerase activity assays performed in HEK293T-TKO cells, along with multi-cycle

https://doi.org/10.1038/s41467-024-55034-y

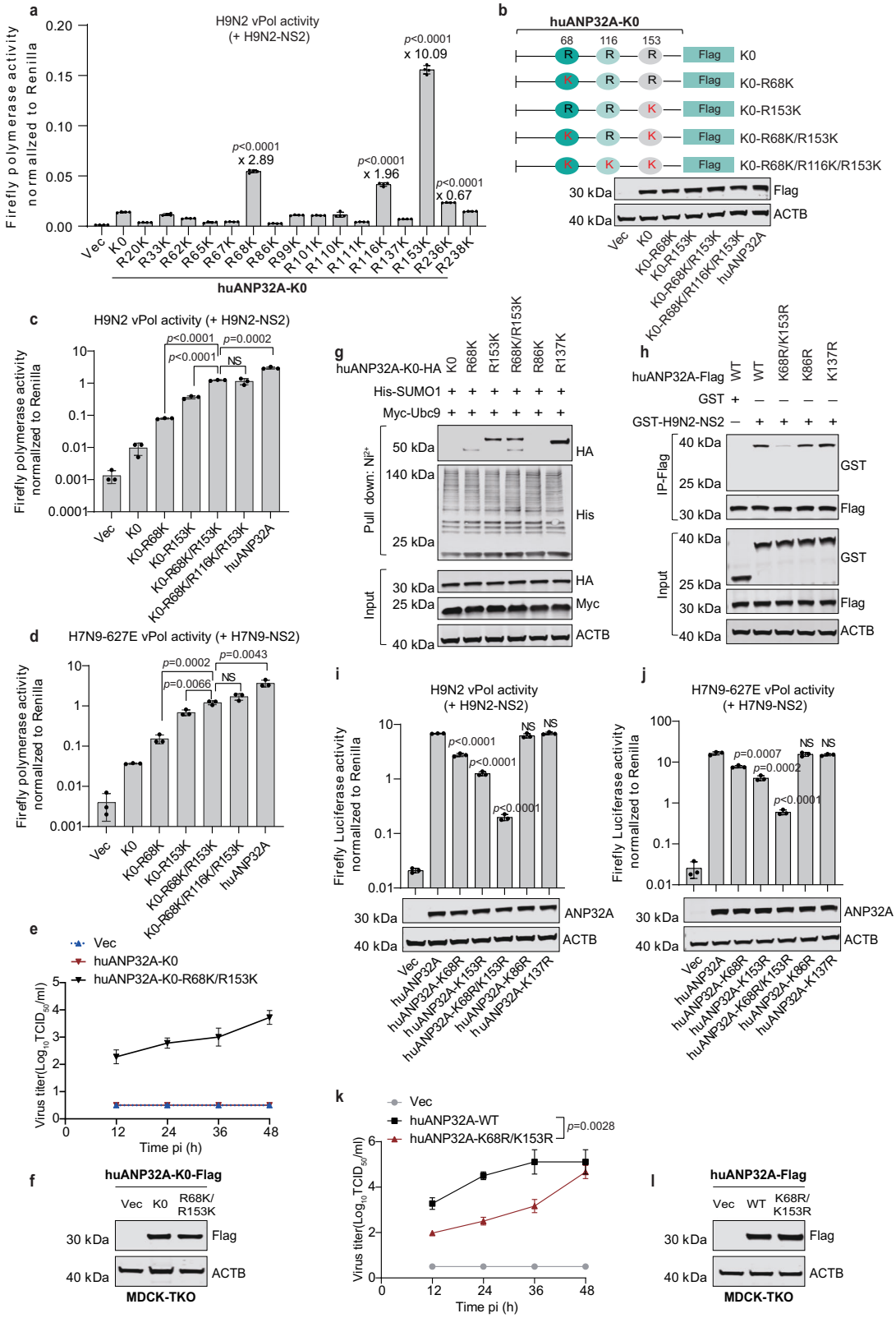

replication assays of the avian H9N2 virus conducted in MDCK-TKO cells, showed that the ability of NS2 to promote huANP32B-K68R/K116R-supported avian vPol activity and viral replication is significantly reduced compared to wild-type huANP32B (Fig. 7i–l). Notably, the introduction of the K-R mutation into either the non-SUMOylated lysine (K67) or the highly SUMOylated lysine (K137) in huANP32B had a limited impact on its interaction with NS2 (Fig. 7h), as well as on the ability of NS2 to enhance huANP32B-supported AIV vPol activity (Fig. 7i, j). This suggests that only site-specific SUMOylation in huANP32B can be recognized by the NS2-SIM.

Intriguingly, the K68R/K116R mutations also did not affect the overall SUMOylation level of huANP32B (Supplementary Fig. 6b). These findings suggest that there are compensatory effects on huANP32B SUMOylation upon the introduction of K68R/K116R

Fig. 6 | The SIM of NS2 binds to the SUMO at the K68/K153 sites of huANP32A. **a** Minigenome assays in HEK293T-TKO cells comparing the effect of the indicated constructs on H9N2 vPol activity. Values above K0 were statistically analyzed using one-way ANOVA followed by a Dunnett's multiple comparisons test against huANP32A-K0 (error bars represent the mean ± SD of $n = 4$ independent biological replicates). **b** Schematic representation of the huANP32A-K0 mutants generated. Western blots demonstrate comparable expression levels for all indicated constructs. **c**, **d** Minigenome assays in HEK293T-TKO cells comparing the effect of the indicated huANP32A-K0 constructs on the H9N2 (**c**) and H7N9 (PB2-627E) (**d**) vPol activity in the presence of NS2. **e** The replication kinetics of the avian H9N2 virus were evaluated in control MDCK-TKO cells or those stably expressing huANP32A-K0-Flag or its mutant (MOI = 0.01), with viral titers determined at the indicated time points. **f** Western blot analysis of MDCK-TKO cells stably reconstituted with the indicated huANP32A-K0-Flag constructs or empty vector. **g** Ni^{2+}-NTA bead affinity pull-down assay showing that the K68 and K153 sites of huANP32A can be modified by SUMO1. **h** Co-IP experiments showing that the K68R/K153R mutations in huANP32A suppress its interaction with H9N2-NS2. **i**, **j** Minigenome assays in HEK293T-TKO cells comparing the effect of the indicated huANP32A constructs on the H9N2 (**i**) and H7N9 (PB2-627E) (**j**) vPol activity. Statistical analyses were performed relative to huANP32A. **k** The replication kinetics of the avian H9N2 virus were evaluated in control MDCK-TKO cells or those stably expressing huANP32A-Flag or huANP32A-K68R/K153R-Flag (MOI = 0.01), with viral titers determined at the indicated time points. **l** Western blot analysis of control MDCK-TKO cells or those stably expressing indicated huANP32A-Flag constructs. In (**c** to **e**) and (**i** to **k**), error bars represent the mean ± SD of $n = 3$ independent biological replicates; NS, not significant; Statistical significance was determined by two-tailed unpaired *t-test* (**c**, **d**, **i** and **j**) or two-way ANOVA (**k**). In (**g**, **h**), experiments were independently repeated three times with consistent results. Source data are provided as a Source Data file.

mutations, further supporting the notion that site-specific SUMOylation of huANP32B mediates its interaction with the SIM in NS2. Interestingly, the K68 and K116 sites are well-conserved among ANP32B proteins from other mammalian species (Supplementary Fig. 7). Immunofluorescence staining indicated that both huANP32B-WT and huANP32B-K68R/K116R mutant predominantly localized in the nucleus (Supplementary Fig. 8b).

Taken together, these data suggest that SUMOylation at K68/K116 of huANP32B mediates its interaction with the SIM in NS2, and this interaction is required for NS2 to promote huANP32B-supported avian vPol activity.

SIM-SUMO-mediated interactions between NS2 and huANP32A/B function to promote avian vPol activity by positively regulating AIV vRNP-huANP32A/B interactions and AIV vRNP assembly

Based on the aforementioned findings, it is evident that the SIM-SUMO-mediated interactions between NS2 and huANP32A/B are indispensable for NS2 to effectively enhance avian vPol activity in human cells. Our previous work has demonstrated that NS2-SIM functions in promoting avian vPol activity by positively regulating vRNP-huANP32A/B interactions and avian vRNP assembly[22]. Building on this, we aimed to further investigate this phenomenon by disrupting the SUMOylation of huANP32A/B, which is crucial for their association with NS2.

We first assessed the impact of huANP32A SUMOylation on H9N2 vRNP-huANP32A interaction in HEK293T-TKO cells reconstituted with the indicated huANP32A-Flag constructs and plasmids encoding H9N2 vRNP. As shown in Fig. 8a, NS2 enhanced the H9N2 vRNP-huANP32A interaction, but failed to enhance H9N2 vRNP-huANP32A-K0 interaction (Fig. 8a, b). However, NS2 effectively promoted the interaction between huANP32A-K0-R68K/R153K and H9N2 vRNP (Fig. 8b). Furthermore, we observed that K68R/K153R mutations impaired the H9N2 vRNP-huANP32A interaction (Fig. 8c). For huANP32B, we performed similar experiments with the H9N2 vRNP and the indicated huANP32B constructs and obtained similar results (Fig. 8d-f).

We proceeded to investigate the impact of huANP32A SUMOylation on the assembly of H9N2 vRNP in HEK293T-TKO cells when reconstituted with the indicated constructs. As shown in Fig. 8g, NS2 enhanced the H9N2 vRNP assembly in HEK293T-TKO cells when reconstituted with wild-type huANP32A, consistent with previous reports[22]. In contrast, NS2 failed to enhance the H9N2 vRNP formation in HEK293T-TKO cells reconstituted with huANP32A-K0 (Fig. 8g, h). However, when HEK293T-TKO cells were reconstituted with huANP32A-K0-R68K/R153K, we observed the enhancement of H9N2 vRNP assembly by the presence of NS2 (Fig. 8h). Furthermore, in the presence of NS2, the level of H9N2 vRNP assembly was reduced when HEK293T-TKO cells were reconstituted with huANP32A-K68R/K153R, as compared to its wild type (Fig. 8i). For huANP32B, we performed similar experiments with the H9N2 vRNP and the indicated huANP32B constructs and obtained similar results (Fig. 8j-l).

Taken together, these data suggest that NS2 employs its SIM to interact with the SUMO of SUMOylated huANP32A/B, and these SIM-SUMO-mediated interactions promote huANP32A/B-supported AIV vPol activity and AIV replication by positively regulating AIV vRNP-huANP32A/B interactions as well as AIV vRNP assembly.

Discussion

As critical cofactors for IAV vPol function, huANP32A/B efficiently support mammalian-adapted IAV vPol activity[11–13,23,31–34]. Nonetheless, huANP32A/B poorly support AIV vPol activity due to the lack of the specific 33 amino-acid insertion found in chANP32A, which serves as the molecular basis for the restriction of avian vPol activity in human cells[11–13,23,33,35,36]. AIVs have evolved various strategies to enable their polymerase to adapt to mammalian ANP32A/B. The predominant strategy used by most AIV strains is the acquisition of adaptive mutations. However, in recent work, we unveiled two previously unidentified strategies[22,37]. The first is that AIVs from avian hosts are able to package avian ANP32A to prime the early stage of viral replication in mammalian cells[37]. The second is that adaptation of the AIV polymerase to huANP32A/B is to some extent promoted with the help of the SIM in NS2[22]. However, the precise mechanism by which the SIM in NS2 promotes mammalian ANP32A/B-supported avian vPol activity remains elusive.

In this study, we continue to elucidate in more detail how NS2 employs its SIM to exert its AIV polymerase-enhancing function. Our findings reveal that NS2 uses its SIM to specifically interact with the SUMO in huANP32A/B. These SIM-SUMO-mediated interactions between NS2 and huANP32A/B are crucial for NS2 to promote avian vPol activity in human cells. We demonstrate that presence of SUMO at K68/K153 sites in huANP32A or K68/K116 sites in huANP32B dictates their binding affinity with NS2-SIM. Furthermore, disrupting the SIM-SUMO interactions between huANP32A/B and NS2, either by interfering with the huANP32A/B SUMOylation or disrupting the integrity of the SIM in NS2, compromises the ability of NS2 to enhance avian vPol activity and AIV replication in human cells. This impairment stems from diminished interactions between AIV vRNP and huANP32A/B and reduced avian vRNP assembly.

SUMO modification is a highly conserved and important post-translational modification[15,16], and plays a pivotal role in regulating diverse viral replication processes[38,39]. In the case of influenza viruses, several studies have shown that SUMOylation regulates viral replication levels and even the ability to spread at different stages of the viral replication cycle[40–44]. However, these investigations have predominantly centered on viral proteins themselves, and knowledge of the influence of SUMO modification of host factors on influenza virus replication remains relatively limited. As indispensable host factors for the function of influenza virus polymerase, huANP32A and huANP32B

https://doi.org/10.1038/s41467-024-55034-y

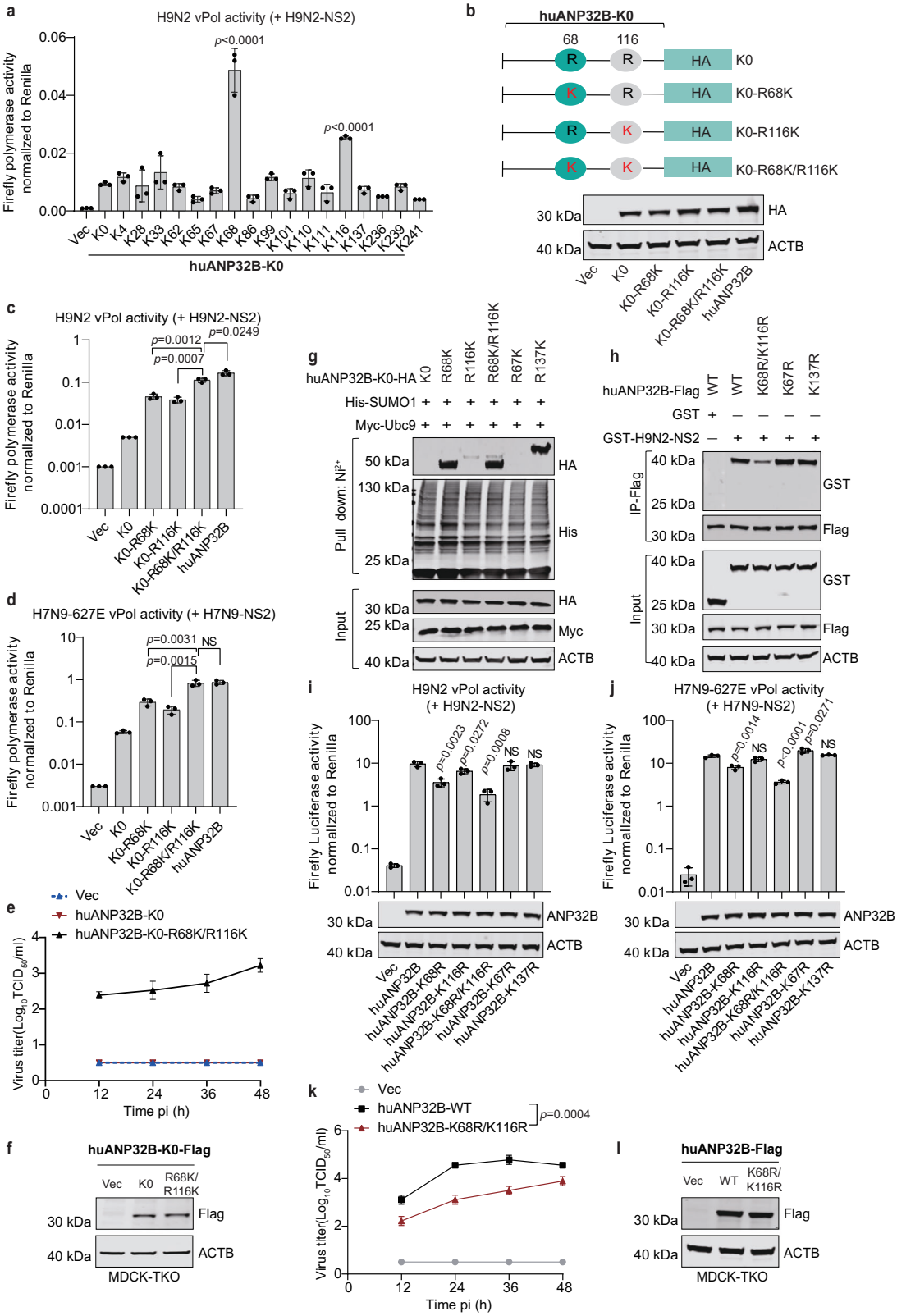

have been identified as potential SUMOylation substrates by large-scale proteomic analysis[24–26]. Here, we provide more evidence that huANP32A and huANP32B undergo SUMOylation, with neither showing a preference for SUMO1, SUMO2 or SUMO3. The SUMOylation process for huANP32A/B is orchestrated by the E3 SUMO ligase PIAS2α and the deSUMOylase SENP1. Consistent with previous findings that huANP32A/B SUMOylation levels increase upon human-adapted IAV infection[24,25], we also observed that huANP32A/B SUMOylation levels were upregulated by H9N2 AIV infection. This suggests that the increase in huANP32A/B SUMOylation following IAV infection is not specific to avian influenza adaptation. However, our findings further indicate that the SIM of NS2 recognizes and binds to SUMO in huANP32A/B. The expression of a NS2 mutant lacking a functional SIM, or huANP32A devoid of the SUMO acceptor K68/K153, or huANP32B

Fig. 7 | The SIM of NS2 binds to the SUMO at the K68/K116 sites of huANP32B. **a** Minigenome assays in HEK293T-TKO cells comparing the effect of indicated huANP32B-K0 constructs on the H9N2 vPol activity. Values higher than K0 were analyzed via one-way ANOVA followed by a Dunnett's multiple comparisons test against huANP32B-K0 (error bars represent the mean ± SD of $n = 3$ independent biological replicates). **b** Schematic representation of the huANP32B-K0 mutants generated. Western blots confirmed comparable expression levels of all constructs. **c**, **d** Minigenome assays in HEK293T-TKO cells comparing the effect of the indicated huANP32B-K0 constructs on the H9N2 (**c**) and H7N9 (PB2-627E) (**d**) vPol activity in the presence of NS2. **e** The replication kinetics of the avian H9N2 virus were evaluated in control MDCK-TKO cells or those stably expressing huANP32B-K0-Flag or its mutant (MOI = 0.01), with viral titers determined at the indicated time points. **f** Western blot analysis of control MDCK-TKO cells or those stably expressing indicated huANP32B-K0-Flag constructs. **g** Ni^{2+}-NTA bead affinity pull-down assay showing that the K68 and K116 sites of huANP32B can be modified by SUMO1. **h** Co-IP experiments showing that the K68R/K116R mutations in huANP32B suppress its interaction with H9N2-NS2. **i**, **j** Minigenome assays in HEK293T-TKO cells comparing the effect of the indicated huANP32B constructs on the H9N2 (**i**) and H7N9 (PB2-627E) (**j**) vPol activity. Statistical analyses were performed relative to huANP32B. **k** The replication kinetics of the avian H9N2 virus were evaluated in control MDCK-TKO cells or those stably expressing huANP32B-Flag or its mutant (MOI = 0.01), with viral titers determined at the indicated time points. **l** Western blot analysis of control MDCK-TKO cells or those stably expressing indicated huANP32B-Flag constructs. In (**c** to **e**) and (**i** to **k**), error bars represent the mean ± SD of $n = 3$ independent biological replicates; NS, not significant; Statistical significance was determined by two-tailed unpaired *t-test* (**c**, **d**, **i** and **j**) or two-way ANOVA (**k**). Experiments in (**g** and **h**) were independently repeated three times with consistent results. Source data are provided as a Source Data file.

lacking the SUMO acceptor K68/K116 all result in an impaired interaction between NS2 and huANP32A/B. Consequently, this reduction compromises the ability of NS2 to enhance huANP32A/B-supported AIV vPol activity. Given that the SIM in NS2 is conserved between avian and human-adapted IAV NS2 proteins, and that human-adapted IAV infection results in increased levels of huANP32A/B SUMOylation, we hypothesised that a potential interaction between human-adapted IAV NS2 and SUMOylated huANP32A/B also exists during the viral replication process. However, we have previously shown that in mammalian cells[22], NS2-regardless of its origin-enhances the function of the avian-signature polymerase, while having a limited effect on the activity of the mammalian-adapted IAV polymerase. This suggests that the role of the SIM-SUMO-mediated interaction between human IAV NS2 and huANP32A/B may be redundant for human IAV polymerase function and requires further investigation.

Previous studies have demonstrated that huANP32A and huANP32B exhibit similar supportive roles in mammalian-adapted IAV vPol activity, and both show limited support for AIV vPol activity[11,12,36]. Despite our discovery in this study of the interaction between NS2 and huANP32A and huANP32B via a similar SIM-SUMO interaction pattern, there are distinctions between the two proteins. Specifically, huANP32A relies on SUMO at K68/K153 for its interaction with NS2-SIM, whereas huANP32B relies on SUMO at K68/K116. Intriguingly, sequence alignment analysis shows the conservation of K68/K116 across mammalian ANP32A/B, whereas K153 conservation is exclusive to mammalian ANP32A. Interestingly, the K68 site, which is conserved in huANP32A, has previously been confirmed as a SUMOylation site in huANP32B through mass spectrometry analysis[26]. While SUMOylation at the K116 site of huANP32A may also influence its interaction with NS2, our findings suggest that its significance is comparatively lower than that at the K68 and K153 sites. In addition, considering the substantial promotion of avian vPol activity by NS2 when supported by other mammalian ANP32A/B, we postulate that the functionality of these sites remains conserved across ANP32A/B from diverse mammalian species. Moreover, given the evolutionary conservation of these SUMOylation residues, we speculate that SUMOylation at these sites in huANP32A/B may also impact their function in supporting mammalian-adapted IAV vPol activity. Further research is necessary to validate this.

While we presented evidence highlighting the crucial role of the SIM-SUMO module in mediating the interaction between NS2 and huANP32A/B, we did not observe a complete disruption of this interaction upon mutation of the SUMO sites in huANP32A/B or the SIM site in NS2. This may be because, as other reports have shown[45], rather than simply facilitating physical contact, SUMOylation may play a fundamental role in structurally orienting the two proteins for closer interaction. This hypothesis is further supported by the observation that both huANP32A-K68R/K153R and huANP32B-K68R/K116R retain comparable SUMOylation levels with their wild-type counterparts, yet still exhibit impaired interaction with NS2-SIM.

The molecular mechanisms underlying the maladaptation of AIV polymerase to huANP32A/B remain largely unknown. Studies using mammalian-adapted influenza virus polymerase subunits have shown that huANP32A/B functions in a manner dependent on its interaction with the trimeric polymerase complex[12,13]. However, some literature suggests that the interaction of huANP32A/B with the trimeric polymerase complex may not be species-specific[23]. The trimeric polymerase complex must associate with viral RNA and NP to form vRNPs, which then control transcription and replication of the viral genome[46]. A substantial body of research suggests that impaired assembly of avian vRNP is associated with the restriction of avian vPol activity in human cells[9,47,48]. Previously, we reported that the enhancement of avian vPol activity by NS2 in human cells occurs through promotion of the assembly of avian vRNP and facilitation of the interaction of vRNP with huANP32A/B[22]. In this study, we provide additional evidence linking the limitation of AIV vPol activity in human cells to compromised AIV vRNP assembly and attenuated interactions with huANP32A/B. We demonstrate that NS2 relies on SIM-SUMO interactions with huANP32A/B to surmount this restriction by fostering interactions between AIV vRNP and huANP32A/B and enhancing AIV vRNP assembly. However, the specific molecular mechanisms governing the role of ANP32A/B in supporting IAV vPol activity remain elusive. Notably, whether the enhanced assembly of avian vRNP precedes increased binding to ANP32A/B or vice versa remains uncertain. Nonetheless, studies have shown that ANP32A/B mediates the assembly of the influenza virus replicase by joining two polymerase molecules to form an asymmetric dimer, thus serving as an essential component of the influenza virus replicase[49–51]. This observation suggests the possibility that increased binding of the AIV vRNP to ANP32A/B may drive enhanced AIV vRNP assembly. Further investigation is required to confirm this.

The SIM typically comprises a central cluster of hydrophobic amino acids, often flanked by acidic or polar residues[18,19]. SIM motifs facilitate non-covalent interactions with mono- or poly-SUMOylated proteins. These SIM-SUMO-mediated interactions exhibit high instability, readily induced or suppressed by altering the SUMOylation status of the involved proteins. Such flexibility confers a survival advantage to cells, enabling swift assembly of protein complexes in response to changing stress conditions, as evidenced by numerous studies[20,52–54]. In this study, we offer additional evidence that, beyond cellular processes, invading viruses such as AIVs use the SIM-SUMO interaction paradigm to engage in host-virus interactions and finely regulate the assembly of protein complexes crucial for viral replication.

Based on our data, we propose a model elucidating the role of NS2 in promoting AIV vPol activity in human cells (Fig. 9). AIV infection induces an elevation in huANP32A/B SUMOylation, subsequently recruiting NS2 through the SIM-SUMO interaction pattern to the nuclear replication platform, where viral genome replication takes place with the assistance of huANP32A/B. The recruited NS2 further

https://doi.org/10.1038/s41467-024-55034-y

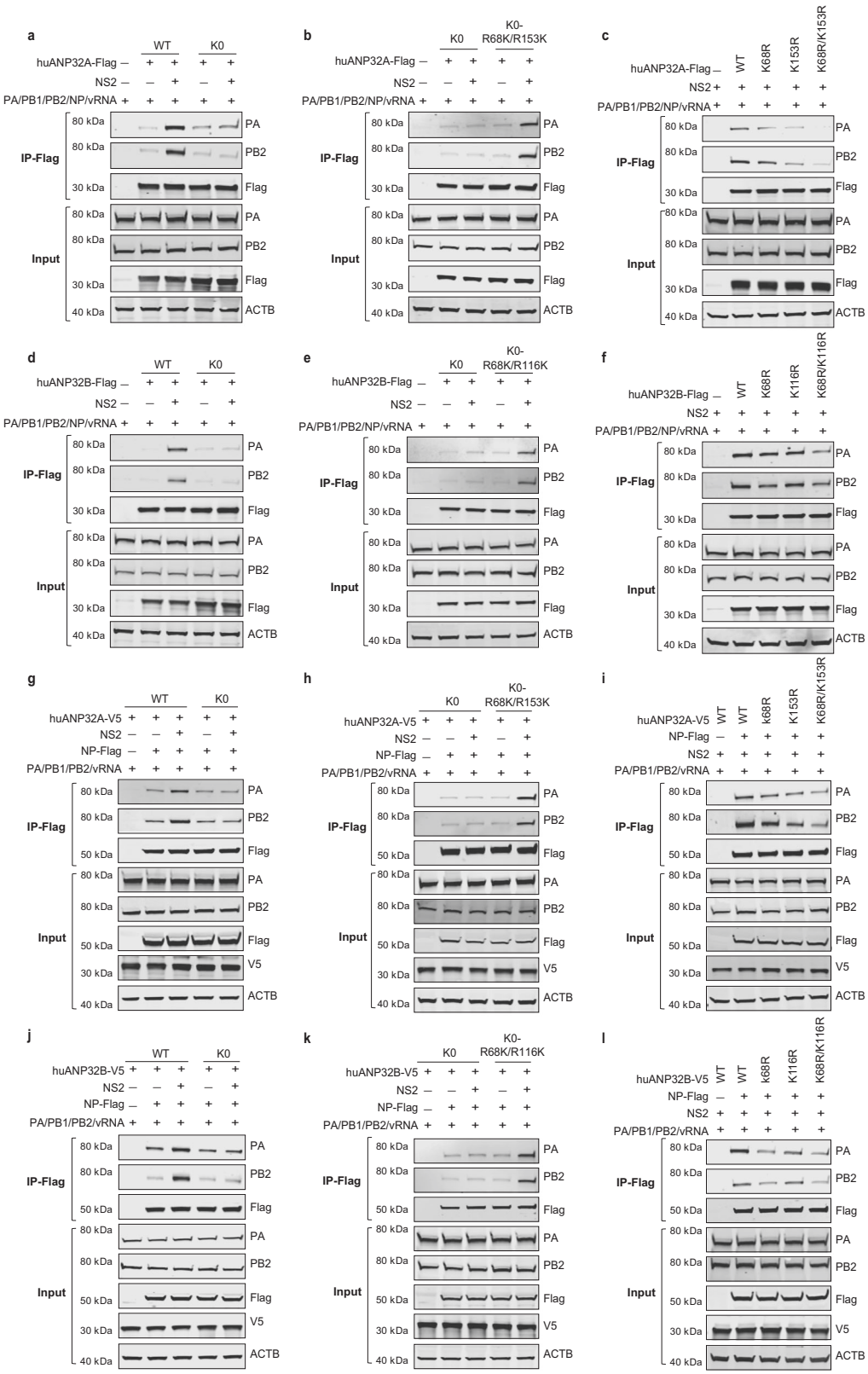

enhances the functionality of huANP32A/B in supporting AIV vPol activity by facilitating the interaction of vRNP with huANP32A/B, thereby augmenting avian vRNP assembly. Given the dynamic and reversible nature of the SUMOylation process, the role of NS2 in promoting huANP32A/B-supported AIV vPol activity can be fine-tuned using this previously unidentified SIM-SUMO operating pattern. Our research contributes to comprehending the intricate interplay among NS2, huANP32A/B, and avian polymerase, shedding light on the molecular mechanism underlying the enhanced adaptation of avian vPol to huANP32A/B conferred by the SIM of NS2. Furthermore, our study delineates a SIM-SUMO dependent mechanism through which the interaction between NS2 and huANP32A/B can be finely modulated by AIVs, allowing them to more effectively adapt to their new mammalian hosts.

Fig. 8 | NS2-SIM enhances avian vPol activity by regulating AIV vRNP-huANP32A/B interactions and AIV vRNP assembly. a NS2 failed to promote the binding of huANP32A-K0 to H9N2 vRNP. HEK293T-TKO cells were transfected with expression vectors for the indicated huANP32A-Flag constructs (0.4 μg), together with H9N2-PB1 (0.4 μg), H9N2-PB2 (0.4 μg), H9N2-PA (0.2 μg), H9N2-NP (0.8 μg), and vRNA luciferase reporter (0.4 μg) and either with or without H9N2-NS2 (50 ng). The transfected cells were collected for IP and western blot analysis 24 hours post-transfection. **b** NS2 promotes huANP32A-K0-R68K/R153K binding to H9N2 vRNP. **c** Effect of K68R, K153R or K68R/K153R mutations in huANP32A on its interaction with H9N2 vRNP in the presence of NS2. **d** NS2 did not enhance huANP32B-K0 binding to H9N2 vRNP. **e** NS2 promotes huANP32B-K0-R68K/R116K binding to H9N2 vRNP. **f** Effect of K68R, K116R or K68R/K116R mutations in huANP32B on its interaction with H9N2 vRNP in the presence of NS2. Experiments in (b to f) were performed as in Fig. 8a. **g** Effect of NS2 on the H9N2 vRNP assembly in HEK293T-TKO cells reconstituted with either huANP32A or huANP32A-K0. HEK293T-TKO cells were transfected with different ANP32A-V5 (0.4 μg), H9N2-NP-Flag (0.8 μg) and polymerase plasmids from H9N2 (0.2 μg PA, 0.4 μg PB1, and 0.4 μg PB2) together with vRNA luciferase reporter (0.4 μg) and H9N2-NS2 (50 ng). After anti-Flag immunoprecipitation at 24 hours post-transfection, the indicated proteins were analyzed with western blotting. **h** Effect of NS2 on the H9N2 vRNP assembly in HEK293T-TKO cells reconstituted with either huANP32A-K0 or huANP32A-K0-R68K/R153K. **i** Measurement of H9N2 vRNP assembly in HEK293T-TKO cells reconstituted with huANP32A or the indicated mutants. **j** Effect of NS2 on H9N2 vRNP assembly in HEK293T-TKO cells reconstituted with either huANP32B or huANP32B-K0. **k** Effect of NS2 on H9N2 vRNP assembly in HEK293T-TKO cells reconstituted with either huANP32B-K0 or huANP32B-K0-R68K/R116K. **l** Measurement of H9N2 vRNP assembly in HEK293T-TKO cells reconstituted with huANP32B or the mutants indicated. Experiments in (**h** to **l**) were performed as in Fig. 8g. Experiments in (**a** to **l**) were independently repeated three times with consistent results. Source data are provided as a Source Data file.

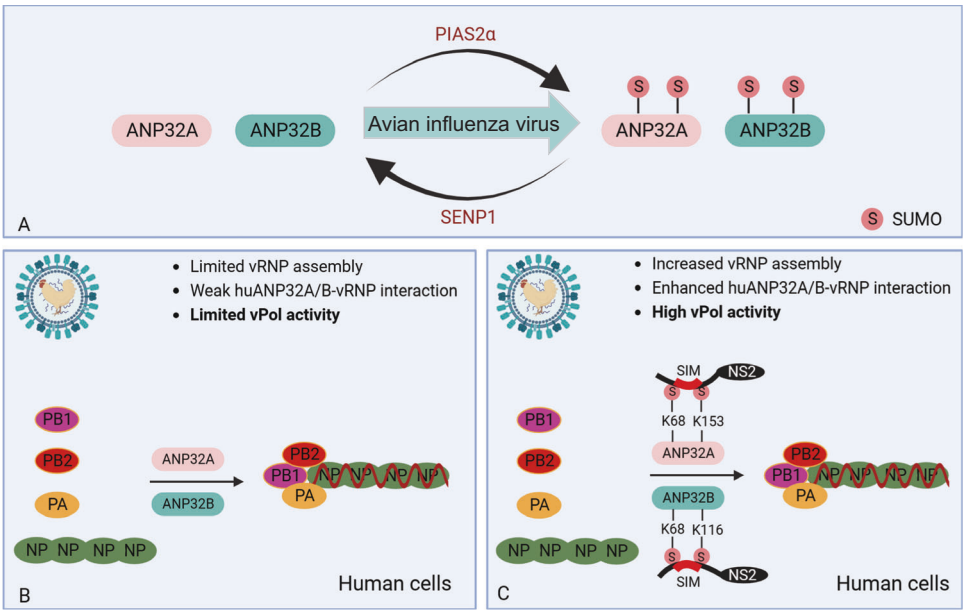

Fig. 9 | Working model illustrating how NS2-SIM promotes huANP32A/B-supported AIV vPol activity. A Both huANP32A and huANP32B are SUMOylated by the E3 SUMO ligase PIAS2α and deSUMOylated by SENP1. SUMOylation of huANP32A and huANP32B increases upon AIV infection. **B** huANP32A and huANP32B cannot efficiently support AIV vPol activity due to weak interactions between AIV vRNP and huANP32A/B, as well as inefficient AIV vRNP assembly. **C** During AIV infection, the NS2 protein is recruited to the replication platform by SUMOylated huANP32A/B via the SIM-SUMO interaction pattern. The recruited NS2 uses its SIM to mediate an intimate association with K68/K153-SUMO in huANP32A or K68/K116-SUMO in huANP32B, which promotes huANP32A/B-supported AIV vPol activity by overcoming the defects in AIV vRNP-huANP32A/B interactions and AIV vRNP assembly. This figure was created with BioRender (https://www.biorender.com).

Methods

Cells, chemical reagents and plasmids

HEK293T cells, the previously described *ANP32A/ANP32B/ANP32E* triple knockout HEK293T cells (HEK293T-TKO)[27], the described *SENP1* knockout HEK293T cells (HEK293T-SENP1-KO), MDCK cells and the described *ANP32A/ANP32B/ANP32E* triple knockout MDCK cells (MDCK-TKO) were cultured in DMEM supplemented with 10% fetal bovine serum (Alphabio, Tianjin Alpha Biotechnology Co., Ltd) and penicillin/streptomycin (100 U/mL). Cells were grown in a 5% CO_2 cell culture incubator at 37 °C.

Puromycin (A1113803) was purchased from Thermo Fisher Scientific. The SUMOylation enzymatic cascade inhibitor subasumstat (TAK-981) was purchased from MedChemExpress (HY-111789).

The reverse genetic system for A/chicken/Zhejiang/B2013/2012 (H9N2) and plasmids pCAGGS-PB1, pCAGGS-PB2, pCAGGS-PA, pCAGGS-NP expressing the RNP components of H9N2 and H7N9 (PB2-627E) have been described previously[12,22,36]. The His-SUMO1/2/3 sequences and their non-conjugatable forms (His-SUMO1m/2 m/3 m) were subcloned separately into a pCEF vector. EGFP-tagged human SUMO1 and its non-conjugatable form, which contains GG-to-AA mutations at the C terminus (EGFP-SUMO1m), were subcloned into a pCAGGS vector. Myc-tagged Ubc9 and V5/Flag-tagged ANP32A/B were subcloned into a pCAGGS vector. VN-Myc-NS2, huANP32A/B-Flag-VC and GST-H9N2-NS2 were also subcloned into a pCAGGS vector. Flag-tagged SENP1, SENP2, SENP3, SENP5, SENP6, SENP7, USPL1, and Flag-tagged PIAS family members, including PIAS1, PIAS2α, PIAS2β, PIAS3 and PIAS4 were subcloned separately into a VR1012 vector. Gene sequences for the lysine-free mutant of huANP32A and huANP32B were generated by gene synthesis and inserted into the pCAGGS vector or VR1012 vector. The indicated additional mutations were introduced using a PCR method and were confirmed by DNA sequencing. For production of lentiviral particles, huANP32A/B and their different mutants were cloned into the lentiviral vector pLVSIN-CMV-PGK-Puro for lentivirus production. All the constructs were subsequently verified by sequencing.

Establishment of MDCK-TKO cells and stable cell lines

The canine *ANP32A*, *ANP32B and ANP32E* genes in MDCK cells were knocked out using the CRISPR-Cas9 system. Briefly, MDCK cells in 6-well

plates were transfected with 1 μg of pMJ920 (Cas9-eGFP) plasmids and 1 μg of gRNA expression plasmids using Polyethylenimine (PEI) reagent. Single green fluorescent protein (GFP)-positive cells were harvested by using fluorescence-activated cell sorting (FACS) after transfection for 36 hours, and were further expanded for screening of monoclonal knockout cell lines with either western blotting or DNA sequencing. Single canine *ANP32A* knockout (AKO) and canine *ANP32B* knockout (BKO) cells were initially generated using two guides targeting the canine *ANP32A* locus and the canine *ANP32B* locus, respectively. Double canine *ANP32A* and *ANP32B* knockout (DKO) cells were then generated using either AKO cells with two guides against canine *ANP32B* locus or BKO cells with two guides against canine *ANP32A* locus. The final triple canine *ANP32A*, *ANP32B* and *ANP32E* knockout MDCK (MDCK-TKO) cells were generated using DKO cells with two guides against canine *ANP32E* locus. AKO cells, BKO cells and DKO cells were validated with western blotting. TKO cells were validated with DNA sequencing. The guide RNAs used in this study are as follows: canine *ANP32A* (TAAGCGATAACAGAATCTCA and CACTTAAATTTAGATGCGTG), canine *ANP32B* (ATAGGTTCGA GAACTTGTCC and AGCCTACATTTATTAAACTG), canine *ANP32E* (TGA CACACAGGCAATTATCA and TAATGTGGAACTAAGTTCAC).

For generation of MDCK-TKO cells stably reconstituted with the different Flag-tagged ANP32A/B constructs, different Flag-tagged ANP32A/B genes were first cloned into a pLVSIN-CMV-PGK-puro vector for producing lentiviral particles in HEK293T cells. MDCK-TKO cells were then infected with the generated lentiviral particles. Puromycin (1 μg/mL) was added 48 hours post-infection to obtain stable cell lines.

Establishment of SENP1 knockout cell lines

The human *SENP1* gene in HEK293T cells was knocked out (designated HEK293T-SENP1-KO) using the CRISPR-Cas9 system. Briefly, HEK293T cells in 6-well plates were transfected with 1 μg of the pMJ920 (Cas9-eGFP) plasmid and 1 μg of gRNA expression plasmids using Polyethylenimine (PEI) reagent. Single green fluorescent protein (GFP)-positive cells were isolated using fluorescence-activated cell sorting (FACS) 36 hours post-transfection and subsequently expanded for the screening of monoclonal knockout cell lines via western blotting (Supplementary Fig. 10). The three guide RNAs utilized in this study are as follows: CCCACCCATGGAGTCGTAAT; ACCATCCGCTTCCG-GAAGTA; GTAAAGATGAGCTTGACGAT.

Virus stock production, and infection assays

Avian H9N2 viruses were rescued in HEK293T cells by using the reverse genetic system of H9N2 and were further inoculated into SPF chicken embryos for propagation, as previously described[36]. The resulting viral stocks were then titrated in MDCK-chANP32A cells. For infection assays, plated cells were infected with H9N2 virus in Opti-MEM supplemented with 1 μg/mL L-1-Tosylamide-2-phenylethyl chloromethyl ketone (TPCK) -trypsin. Cell supernatants were collected at the indicated time points, and virus titers were determined in MDCK-chANP32A cells using 50% tissue culture infective dose ($TCID_{50}$) assay.

Minigenome assays

HEK293T-TKO cells were plated in 24-well plates and co-transfected with the following plasmids: pPolI-luc (40 ng), pRL-TK encoding Renilla luciferase (5 ng), pCAGGS-PB1 (20 ng), pCAGGS-PB2 (20 ng), pCAGGS-PA (10 ng), pCAGGS-NP (40 ng), and plasmids encoding the indicated ANP32 proteins (20 ng), along with or without the plasmid encoding NS2, using Polyethylenimine (PEI) transfection reagent. Twenty-four hours post-transfection, the cells were lysed, and relative luciferase activity was measured using the Dual-luciferase system (Promega) with a Berthold Centro LB 960 microplate luminometer.

Immunoprecipitation assays

Cells were lysed with lysis buffer (50 mM Hepes-NaOH [pH 7.9], 100 mM NaCl, 50 mM KCl, 0.25% NP-40, and 1 mM DTT) plus complete inhibitor cocktail (APExBIO, Houston, USA, K1007). The lysates were centrifuged (13000 g, 10 min). The supernatants were incubated with anti-Flag M2 magnetic beads (Sigma-Aldrich, M8823) at 4 °C overnight. The beads were washed five times with PBS and eluted with 3× Flag peptide (APExBIO, Houston, USA; A6001) and the immunoprecipitated proteins were then analyzed using western blotting.

Mass spectrometry analysis

Proteomic analysis was performed by Genechem Biotechnology Co., Ltd. (Shanghai, China) on three independent samples from the Flag-H9N2-NS2 group (Flag1, Flag2, Flag3) and three independent samples from the control vector group (V1, V2, V3). The analysis utilized a nanoElute (Bruker, Bremen, Germany) coupled with a timsTOF Pro mass spectrometer (Bruker, Bremen, Germany) equipped with a CaptiveSpray source. Peptides were separated on a 25 cm×75 μm analytical column, 1.6 μm C18 beads with a packed emitter tip (IonOpticks, Australia). The column temperature was maintained at 50 °C using an integrated column oven (Sonation GmbH, Germany). The column was equilibrated with 4 column volumes before loading the sample in 100% buffer A (99.9% MilliQ water, 0.1% FA) (both steps performed at 800 bar). Samples were separated at 300 nl/min using a linear gradient as follows 1.5 hour gradient: 2-22% buffer B for 75 min, 22-37% buffer B for 5 min, 37-80% buffer B for 5 min, held in 80% buffer B for 5 min.The timsTOF Pro (Bruker, Bremen, Germany) was operated in PASEF mode. Mass range 100 to 1700 m/z, 1/K0 start 0.75 V·s/cm2 end 1.4 V·s/cm2, ramp time 100 ms, lock duty cycle 100%, capillary voltage 1500 V, dry gas 3 l/min, dry temp 180 °C, PASEF settings: 10 MS/MS scans (total cycle time 1.16 sec), loading range 0-5, active exclusion for 0.5 min, scheduling Target intensity 10000, intensity threshold 2500, CID collision energy 20-59 eV. MS data were analyzed using MaxQuant software version 1.6.17.0. MS data were searched against the human protein database (uniprot_homo_20240515_20435_9606_swiss_prot). An initial search was performed with a precursor mass window of 10 ppm. The search followed an enzymatic cleavage rule of trypsin/P, allowing a maximum of three missed cleavage sites and a mass tolerance of 40 ppm for fragment ions. Carbamidomethylation of cysteines was defined as a fixed modification, while protein N-terminal acetylation and methionine oxidation were defined as variable modifications for database searching. In addition, the MS data were also searched against the viral proteins of A/chicken/Zhejiang/B2013/2012(H9N2). The global false discovery rate (FDR) cut-off for peptide and protein identification was set at 0.01.

In vitro SUMOylation assays

HEK293T cells grown in 75 cm^2 cell culture flasks were transfected with the indicated plasmids. Transfected cells were lysed in 2 mL RIPA lysis buffer supplemented with 1% SDS, 10 mM N-Ethylmaleimide (NEM) (Sigma-Aldrich, E3876) and complete inhibitor cocktail (APExBIO, Houston, USA, K1007). The lysates were sonicated until they became fluid and then centrifuged (13000 g, 10 min). The supernatants were incubated with Ni^{2+}-NTA beads (Sangon Biotech, C650033) at 4 °C overnight. The beads were then washed sequentially with buffer A (50 mM Tris-HCl, 0.5 M NaCl, 6 M guanidine-HCl), buffer B (50 mM Tris-HCl, 0.5 M NaCl, 8 M urea), and PBS. The bound proteins were then eluted with elution buffer containing 200 mM imidazole, and analyzed with western blotting. SUMOylation assays, shown in Figs. 6g and 7g, were conducted in HEK293T-SENP1-KO cells.

siRNA treatment

siRNA transfection was performed using Lipofectamine™ 2000 transfection reagent according to the manufacturer's protocol on the same day as HEK293T cells were seeded. 24 hours after siRNA transfection, the cells were further transfected with plasmids as indicated using Polyethylenimine (PEI) transfection reagent. Cells were harvested for analysis 24 hours after the second transfection step. siRNA

oligonucleotides against SENP1 (siRNA1: 5′-GCGCCAGAUUGAAGAACAGAA-3′; siRNA2: 5′-UGACCAUUACACGCAAAGAUA-3′), PIAS2(siRNA1:5′-GCCAUGUUAUUACAGAGAUUA-3′;siRNA2:5′-GCUGCUAUUCCGCCUUCAUUA-3′) and non-targeting control (5′-UUCUCCGAACGUGUCACGU-3′) were purchased from Seven Innovation (China, Beijing) Biotechnology.

Western blot analysis

Western blot analysis was conducted following established protocols[12] using the following antibodies: rabbit anti-Flag (Sigma, F7425), mouse anti-Flag (Sigma, F1804), rabbit anti-HA (Sigma, H6908), rabbit anti-ACTB (Abclonal, AC026), mouse anti-ACTB (Abclonal, AC004), rabbit anti-Myc (Abclonal, AE070), rabbit anti-SUMO1 (Abclonal, A19121), rabbit anti-SUMO2/3 (Abclonal, A5066), rabbit anti-SENP1(Abcam, ab108981), mouse anti-His (Proteintech, 66005-1-Ig), rabbit anti-V5 (Proteintech, 14440-1-AP), rabbit anti-SENP1 (Proteintech, 25349-1-AP), rabbit anti-PIAS2 (Proteintech, 16074-1-AP), rabbit anti-GST (Proteintech, 10000-0-AP), rabbit anti-ANP32A (Proteintech,15810-1-AP), rabbit anti-ANP32B (Proteintech, 10843-1-AP), mouse anti-ANP32A (Proteintech, 67687-1-Ig), mouse anti-ANP32B (Proteintech, 66160-1-Ig), rabbit anti-influenza A virus NS2 (GeneTex, GTX125953), rabbit anti-influenza B virus NP (GeneTex, GTX128538), rabbit anti-influenza A virus PB2 (GeneTex, GTX125926), rabbit anti-influenza A virus PA (GeneTex, GTX118991), mouse anti-influenza A virus PA (prepared in our laboratory, 1:5000 for WB), mouse anti-influenza A virus NP (prepared in our laboratory, 1:5000 for WB), Biotin-conjugated Affinipure Goat Anti-Rabbit IgG(H + L) (Proteintech, SA00004-2), DyLight 800-labeled Anti-Mouse IgG (H + L) Antibody (KPL, 5230-0415), DyLight 680-labeled Anti-Rabbit IgG (H + L) Antibody (KPL, 5230-0402) and DyLight™ 680-labeled streptavidin (KPL, 5270-0025).

To detect NS2-huANP32A/B interactions, the GST-NS2 signal within purified protein complexes was enhanced using the biotin-streptavidin system. Specifically, the membrane underwent sequential incubation with anti-GST (rabbit) antibody, Biotin-conjugated Affinipure goat anti-Rabbit IgG (H + L), and DyLight™ 680-labelled streptavidin. Subsequently, bands were analyzed by scanning blots with the Odyssey Imaging System (Li-Cor, Lincoln, NE, USA).

Generation of stable cell lines

HIV-1-based lentiviral particles were produced by transfecting HEK293T cells with plasmids pspAX2, pMD2.0 G and vector plasmids (pLVSIN-CMV-PGK-puro). Supernatants were collected 48 h post-transfection. Then HEK293T-TKO cells were then infected with these generated lentiviruses. Stable cell lines were subjected to puromycin selection (1 μg/mL).

Immunofluorescence staining

Immunofluorescence analysis was performed as previously described[55]. Briefly, the indicated cells were fixed in 4% paraformaldehyde for 20 min, followed by permeabilization in PBS containing 0.05% Triton X-100 for 10 min. The cells were then blocked in PBS with 5% milk powder in PBS for 30 min before incubation with primary antibodies at 4 °C overnight. The cells were then washed three times with PBS before incubation with Alexa Fluor 488 (Invitrogen, A11029)-, 405 (Invitrogen, A31553)-, or 647 (Invitrogen, A32733)-conjugated secondary antibodies, with or without DAPI, for 1 hour at room temperature. Images were acquired using a confocal microscope (Carl Zeiss LSM 800 Confocal Microscope and ZEN 2.3 LITE software).

Proximity-ligation assay (PLA)

PLA experiments were conducted using the Duolink In Situ Red Starter Kit (mouse/rabbit, Sigma-Aldrich, cat. no. DUO92101) to identify direct interactions between two proteins. Briefly, HEK293T cells were seeded in Nunc glass-bottom dishes. After treatment (with or without H9N2 infection), the cells were fixed in 4% paraformaldehyde and permeabilized with 0.1% Triton X-100, followed by blocking with Duolink® PLA Blocking Buffer. A pair of primary antibodies derived from mouse and rabbit was incubated overnight at 4 °C, then washed twice with 1x Duolink In Situ Wash Buffer A for 5 minutes each, followed by incubation with Duolink® anti-rabbit PLUS and anti-mouse MINUS PLA probes for 1 hour. After washing twice with 1x Duolink In Situ Wash Buffer A for 5 minutes each, a ligation-ligase solution was added and incubated at 37 °C for 30 minutes. The samples were then washed twice for 5 minutes, followed by amplification with polymerase solution at 37 °C for 100 minutes, and finally washed twice with 1x Duolink In Situ Wash Buffer B for 10 minutes each. The samples were mounted with Duolink In Situ Mounting Medium containing DAPI and imaged using a confocal microscope. Control experiments were conducted with each primary antibody incubated separately to validate the specificity of the assay. Protein-protein interactions appeared as red dots.

Bimolecular fluorescence complementation (BiFC) Assay

For BiFC visualization, HEK293T cells were cultured on glass-bottom cell culture dishes and transiently transfected with VN and VC expression vectors. After 24 hours, the cells were fixed with 4% paraformaldehyde, permeabilized with 0.1% Triton X-100, and blocked with 5% bovine serum albumin (BSA). They were then incubated with the corresponding primary antibodies at 4 °C overnight, followed by Alexa Fluor 405- or 647-conjugated secondary antibodies for 1 hour at room temperature in the dark. Finally, the cells were washed with PBS five times and either treated with DAPI reagent or left untreated. Samples were assessed using confocal microscopy (Carl Zeiss LSM 800 Confocal Microscope and ZEN 2.3 LITE software).

For BiFC analysis using flow cytometry, HEK293T cells were seeded in 24-well plates and transfected with VN and/or VC expression vectors. After 24 hours, the cells were gently trypsinized and collected into 15 ml Falcon tubes. The cells were then pelleted by centrifugation, washed twice with ice-cold phosphate-buffered saline (PBS), and resuspended in 100 μl of PBS. Fluorescence-activated cell sorting (FACS) analysis was conducted with an excitation wavelength of 488 nm, following the gating strategy outlined in Supplementary Fig. 11. Suspensions containing 1×10^4 cells were analyzed for the mean fluorescence intensity (MFI) of the BiFC fluorescence signals from the transfected cells.

RNA isolation and real-time quantitative PCR

Total RNA was isolated from cells using a RNeasy mini kit (Qiagen, 74106) according to the manufacturer's instructions. Complementary DNA was synthesized using the PrimeScript RT reagent kit with a gDNA Eraser (Takara, RR047B) according to the manufacturer's instructions. The mRNA level of PIAS2 in HEK293T cells was quantified using SYBR-Green (Takara, RR430A)-based real-time quantitative PCR analysis. Real-time PCR was performed using the human PIAS2 mRNA primers: PIAS2-qPCR-F: 5′-GTTCTTGGTGTCCAATGAGACCG-3′; PIAS2-qPCR-R: 5′-TGCTTGCCTCACTGGCTACAGT-3′. ACTB was used as a housekeeping control to normalize the number of living cells. The ACTB primers were ACTB-forward (5′-ACGGCATCGTCACCAACTG-3′) and ACTB-reverse (5′-CAAACATGATCTGGGTCATCTTCTC-3′).

Statistics and reproducibility

All statistical analyses were performed with GraphPad Prism software. Quantitative data are presented as mean ± SD and statistical significance was analysed using two-tailed unpaired t-test, two-way ANOVA or one-way ANOVA followed by Dunnett's multiple comparisons tests, where appropriate, as indicated in the figure legends. A p-value of 0.05 or less was considered statistically significant. For all bar graphs, data are presented as mean ± SD from at least three independent biological replicates ($n \geq 3$). Fluorescence images in Figs. 1e, 1g, 1i; 3c, 3f, 3j, 3m are representative of two independent experiments with

similar results. Western blot images in Fig. 5i and k were carried out once to validate the comparable expression levels of indicated constructs in transfected MDCK-TKO cells, which were used for the experiments shown in Fig. 5h and j, respectively. Western blot images in Figs. 6f, 6l; and 7f, 7l were carried out once to validate the comparable expression levels of overexpressed proteins in MDCK-TKO stable cell lines, which were then used for the experiments shown in Figs. 6e, 6k; and 7e, 7k, respectively. Western blot images in Figs. 6b and 7b were carried out once to validate the comparable expression levels of the indicated constructs, which were then used for the experiments shown in Figs. 6c, 6d; 7c, 7d, respectively. All other Western blots were independently repeated at least twice with consistent results; the exact number of repetitions is provided in the figure legends.

Reporting summary

Further information on research design is available in the Nature Portfolio Reporting Summary linked to this article.

Data availability

The mass spectrometry proteomics data have been deposited to the ProteomeXchange Consortium (https://proteomecentral.proteomexchange.org) via the iProX partner repository[56,57] with the dataset identifier PXD056322. All data supporting the findings of this study are available within the paper and its source data files. Source data are provided with this paper.

References

1. Long, J. S., Mistry, B., Haslam, S. M. & Barclay, W. S. Host and viral determinants of influenza A virus species specificity. *Nat Rev Microbiol.* **17**, 67–81 (2019).
2. Kuiken, T. et al. Host species barriers to influenza virus infections. *Science.* **312**, 394–397 (2006).
3. Cauldwell, A. V., Long, J. S., Moncorge, O. & Barclay, W. S. Viral determinants of influenza A virus host range. *J Gen Virol.* **95**, 1193–1210 (2014).
4. Neumann, G. & Kawaoka, Y. Transmission of influenza A viruses. *Virology.* **479-480**, 234–246 (2015).
5. Naffakh, N., Tomoiu, A., Rameix-Welti, M. A. & van der Werf, S. Host restriction of avian influenza viruses at the level of the ribonucleoproteins. *Annu Rev Microbiol.* **62**, 403–424 (2008).
6. Almond, J. W. A single gene determines the host range of influenza virus. *Nature.* **270**, 617–618 (1977).
7. Subbarao, E. K., London, W. & Murphy, B. R. A single amino acid in the PB2 gene of influenza A virus is a determinant of host range. *J Virol.* **67**, 1761–1764 (1993).
8. Gao, Y. et al. Identification of amino acids in HA and PB2 critical for the transmission of H5N1 avian influenza viruses in a mammalian host. *PLoS Pathog.* **5**, e1000709 (2009).
9. Mehle, A. & Doudna, J. A. An inhibitory activity in human cells restricts the function of an avian-like influenza virus polymerase. *Cell Host Microbe.* **4**, 111–122 (2008).
10. Moncorge, O., Mura, M. & Barclay, W. S. Evidence for avian and human host cell factors that affect the activity of influenza virus polymerase. *J Virol.* **84**, 9978–9986 (2010).
11. Long, J. S. et al. Species difference in ANP32A underlies influenza A virus polymerase host restriction. *Nature.* **529**, 101–104 (2016).
12. Zhang, H. et al. Fundamental Contribution and Host Range Determination of ANP32A and ANP32B in Influenza A Virus Polymerase Activity. *J. Virol.* **93**, e00174-19 (2019).
13. Long, J. S. et al. Species specific differences in use of ANP32 proteins by influenza A virus. *Elife.* **8**, e45066 (2019).
14. Geiss-Friedlander, R. & Melchior, F. Concepts in sumoylation: a decade on. *Nat Rev Mol Cell Biol.* **8**, 947–956 (2007).
15. Celen, A. B. & Sahin, U. Sumoylation on its 25th anniversary: mechanisms, pathology, and emerging concepts. *FEBS J.* **287**, 3110–3140 (2020).
16. Vertegaal, A. C. O. Signalling mechanisms and cellular functions of SUMO. *Nat Rev Mol Cell Biol.* **23**, 715–731 (2022).
17. Song, J., Durrin, L. K., Wilkinson, T. A., Krontiris, T. G. & Chen, Y. Identification of a SUMO-binding motif that recognizes SUMO-modified proteins. *Proc Natl Acad Sci USA.* **101**, 14373–14378 (2004).
18. Lascorz, J., Codina-Fabra, J., Reverter, D. & Torres-Rosell, J. SUMO-SIM interactions: From structure to biological functions. *Semin Cell Dev Biol.* **132**, 193–202 (2022).
19. Yau, T. Y., Sander, W., Eidson, C. & Courey, A. J. SUMO Interacting Motifs: Structure and Function. *Cells.* **10**, 2825 (2021).
20. Moriuchi, T. & Hirose, F. SUMOylation of RepoMan during late telophase regulates dephosphorylation of lamin A. *J. Cell Sci.* **134**, jcs247171 (2021).
21. Manz, B., Brunotte, L., Reuther, P. & Schwemmle, M. Adaptive mutations in NEP compensate for defective H5N1 RNA replication in cultured human cells. *Nat Commun.* **3**, 802 (2012).
22. Sun, L. et al. The SUMO-interacting motif in NS2 promotes adaptation of avian influenza virus to mammals. *Sci Adv.* **9**, eadg5175 (2023).
23. Domingues, P. & Hale, B. G. Functional Insights into ANP32A-Dependent Influenza A Virus Polymerase Host Restriction. *Cell Rep.* **20**, 2538–2546 (2017).
24. Domingues, P. et al. Global Reprogramming of Host SUMOylation during Influenza Virus Infection. *Cell Rep.* **13**, 1467–1480 (2015).
25. Schmidt, N. et al. An influenza virus-triggered SUMO switch orchestrates co-opted endogenous retroviruses to stimulate host antiviral immunity. *Proc Natl Acad Sci USA.* **116**, 17399–17408 (2019).
26. Hendriks, I. A., D'Souza, R. C., Yang, B., Verlaan-de Vries, M., Mann, M. & Vertegaal, A. C. Uncovering global SUMOylation signaling networks in a site-specific manner. *Nat Struct Mol Biol.* **21**, 927–936 (2014).
27. Zhang, Z. et al. Selective usage of ANP32 proteins by influenza B virus polymerase: Implications in determination of host range. *PLoS Pathog.* **16**, e1008989 (2020).
28. Pal, S., Santos, A., Rosas, J. M., Ortiz-Guzman, J. & Rosas-Acosta, G. Influenza A virus interacts extensively with the cellular SUMOylation system during infection. *Virus Res.* **158**, 12–27 (2011).
29. Kunz, K., Piller, T. & Muller, S. SUMO-specific proteases and isopeptidases of the SENP family at a glance. *J. Cell Sci.* **131**, jcs211904 (2018).
30. Gareau, J. R. & Lima, C. D. The SUMO pathway: emerging mechanisms that shape specificity, conjugation and recognition. *Nat Rev Mol Cell Biol.* **11**, 861–871 (2010).
31. Staller, E. et al. ANP32 proteins are essential for influenza virus replication in human cells. *J. Virol.* **93**, e00217-19 (2019).
32. Baker, S. F., Ledwith, M. P. & Mehle, A. Differential Splicing of ANP32A in Birds Alters Its Ability to Stimulate RNA Synthesis by Restricted Influenza Polymerase. *Cell Rep.* **24**, 2581–2588.e2584 (2018).
33. Bi, Z. et al. Insights into species-specific regulation of ANP32A on the mammalian-restricted influenza virus polymerase activity. *Emerg Microbes Infect.* **8**, 1465–1478 (2019).
34. Domingues, P. et al. Profiling host ANP32A splicing landscapes to predict influenza A virus polymerase adaptation. *Nat Commun.* **10**, 3396 (2019).
35. Peacock, T. P. et al. Swine ANP32A Supports Avian Influenza Virus Polymerase. *J. Virol.* **94**, e00132-20 (2020).
36. Zhang, H. et al. A unique feature of swine ANP32A provides susceptibility to avian influenza virus infection in pigs. *PLoS Pathog.* **16**, e1008330 (2020).

37. Na, L. et al. Avian ANP32A incorporated in avian influenza A virions promotes interspecies transmission by priming early viral replication in mammals. *Sci Adv*. **10**, eadj4163 (2024).
38. Imbert, F. & Langford, D. Viruses, SUMO, and immunity: the interplay between viruses and the host SUMOylation system. *J Neurovirol*. **27**, 531–541 (2021).
39. Fan, Y. et al. SUMOylation in Viral Replication and Antiviral Defense. *Adv Sci (Weinh)*. **9**, e2104126 (2022).
40. Wu, C. Y., Jeng, K. S. & Lai, M. M. The SUMOylation of matrix protein M1 modulates the assembly and morphogenesis of influenza A virus. *J Virol*. **85**, 6618–6628 (2011).
41. Han, Q. et al. Sumoylation of influenza A virus nucleoprotein is essential for intracellular trafficking and virus growth. *J Virol*. **88**, 9379–9390 (2014).
42. Li, J. et al. Viral RNA-binding ability conferred by SUMOylation at PB1 K612 of influenza A virus is essential for viral pathogenesis and transmission. *PLoS Pathog*. **17**, e1009336 (2021).
43. Guo, J. et al. SUMOylation of Matrix Protein M1 and Filamentous Morphology Collectively Contribute to the Replication and Virulence of Highly Pathogenic H5N1 Avian Influenza Viruses in Mammals. *J Virol*. **96**, e0163021 (2022).
44. Wang, G. et al. PIAS1-mediated SUMOylation of influenza A virus PB2 restricts viral replication and virulence. *PLoS Pathog*. **18**, e1010446 (2022).
45. Verma, V. et al. SUMO enables substrate selectivity by mitogen-activated protein kinases to regulate immunity in plants. *Proc. Natl Acad. Sci. USA*. **118**, e2021351118 (2021).
46. Wandzik, J. M., Kouba, T. & Cusack, S. Structure and Function of Influenza Polymerase. *Cold Spring Harb. Perspect. Med*. **11**, a038372 (2021).
47. Labadie, K., Dos Santos Afonso, E., Rameix-Welti, M. A., van der Werf, S. & Naffakh, N. Host-range determinants on the PB2 protein of influenza A viruses control the interaction between the viral polymerase and nucleoprotein in human cells. *Virology*. **362**, 271–282 (2007).
48. Rameix-Welti, M. A., Tomoiu, A., Dos Santos Afonso, E., van der Werf, S. & Naffakh, N. Avian Influenza A virus polymerase association with nucleoprotein, but not polymerase assembly, is impaired in human cells during the course of infection. *J Virol*. **83**, 1320–1331 (2009).
49. Carrique, L. et al. Host ANP32A mediates the assembly of the influenza virus replicase. *Nature*. **587**, 638–643 (2020).
50. Staller, E. et al. Structures of H5N1 influenza polymerase with ANP32B reveal mechanisms of genome replication and host adaptation. *Nat Commun*. **15**, 4123 (2024).
51. Arragain, B. et al. Structures of influenza A and B replication complexes give insight into avian to human host adaptation and reveal a role of ANP32 as an electrostatic chaperone for the apo-polymerase. *Nat Commun*. **15**, 6910 (2024).
52. Dorison, H., Talhaoui, I. & Mazon, G. SUMO-mediated recruitment allows timely function of the Yen1 nuclease in mitotic cells. *PLoS Genet*. **18**, e1009860 (2022).
53. Psakhye, I. & Jentsch, S. Protein group modification and synergy in the SUMO pathway as exemplified in DNA repair. *Cell*. **151**, 807–820 (2012).
54. Jentsch, S. & Psakhye, I. Control of nuclear activities by substrate-selective and protein-group SUMOylation. *Annu Rev Genet*. **47**, 167–186 (2013).
55. Guo, X. et al. A/(H1N1) pdm09 NS1 promotes viral replication by enhancing autophagy through hijacking the IAV negative regulatory factor LRPPRC. *Autophagy*. 1-18 (2022).
56. Chen, T. et al. iProX in 2021: connecting proteomics data sharing with big data. *Nucleic Acids Res*. **50**, D1522–D1527 (2022).
57. Ma, J. et al. iProX: an integrated proteome resource. *Nucleic Acids Res*. **47**, D1211–D1217 (2019).

Acknowledgements

We thank Dr. Zejun Li (Shanghai Veterinary Research Institute, CAAS) for providing plasmids. We thank former lab members Zhenyu Zhang and Jiaqi Han for their help in the preparation of the MDCK-TKO cells. We thank Professor Hualan Chen for providing the plasmids and for her helpful discussions. This work was supported by the National Natural Science Foundation of China (32330103) to X.J.W., the National Natural Science Foundation of China (32302959) to L.K.S., and the Natural Science Foundation of Heilongjiang Province of China (TD2022C006) to X.J.W.

Author contributions

X.J.W. designed and supervised the study and revised the manuscript. L.K.S. and X.J.W. analyzed the data and designed the study. L.K.S. wrote the original draft and performed the experiments. X.G. assisted with data validation. M.M.Y. and H.L.R. assisted with sample collection. X-F.W. assisted with manuscript editing. All authors reviewed the manuscript.

Competing interests

The authors declare no competing interests.

Additional information

Supplementary information The online version contains supplementary material available at https://doi.org/10.1038/s41467-024-55034-y.

Correspondence and requests for materials should be addressed to Xiaojun Wang.

Peer review information *Nature Communications* thanks the anonymous, reviewer(s) for their contribution to the peer review of this work. A peer review file is available.